Emergence of sex-specific transcriptomes in a sexually dimorphic brain nucleus

Samantha R. Friedrich[1], **Alexander A. Nevue**[1], **Abraão L.P. Andrade**[2], **Tarciso A.F. Velho**[2], **Claudio V. Mello**[1,3,*]

[1]Department of Behavioral Neuroscience, Oregon Health & Science University (OHSU), Portland, OR 97239, USA

[2]Brain Institute, Federal University of Rio Grande do Norte, Natal, RN 59078-970, Brazil

[3]Lead contact

SUMMARY

We present the transcriptomic changes underlying the development of an extreme neuroanatomical sex difference. The robust nucleus of the arcopallium (RA) is a key component of the songbird vocal motor system. In zebra finch, the RA is initially monomorphic and then atrophies in females but grows up to 7-fold larger in males. Mirroring this divergence, we show here that sex-differential gene expression in the RA expands from hundreds of predominantly sex chromosome Z genes in early development to thousands of predominantly autosomal genes by the time sexual dimorphism asymptotes. Male-specific developmental processes include cell and axonal growth, synapse assembly and activity, and energy metabolism; female-specific processes include cell polarity and differentiation, transcriptional repression, and steroid hormone and immune signaling. Transcription factor binding site analyses support female-biased activation of pro-apoptotic regulatory networks. The extensive and sex-specific transcriptomic reorganization of RA provides insights into potential drivers of sexually dimorphic neurodevelopment.

In brief

Friedrich et al. demonstrate extensive transcriptomic sex differences underlying the sexually dimorphic development of vocal nucleus RA in the songbird brain. They find sex-specific gene regulation linked to distinct biological processes, developmental shifts in the relative signal from

sex chromosome to autosomal genes, and evidence of female-biased pro-apoptotic regulatory networks.

Graphical Abstract
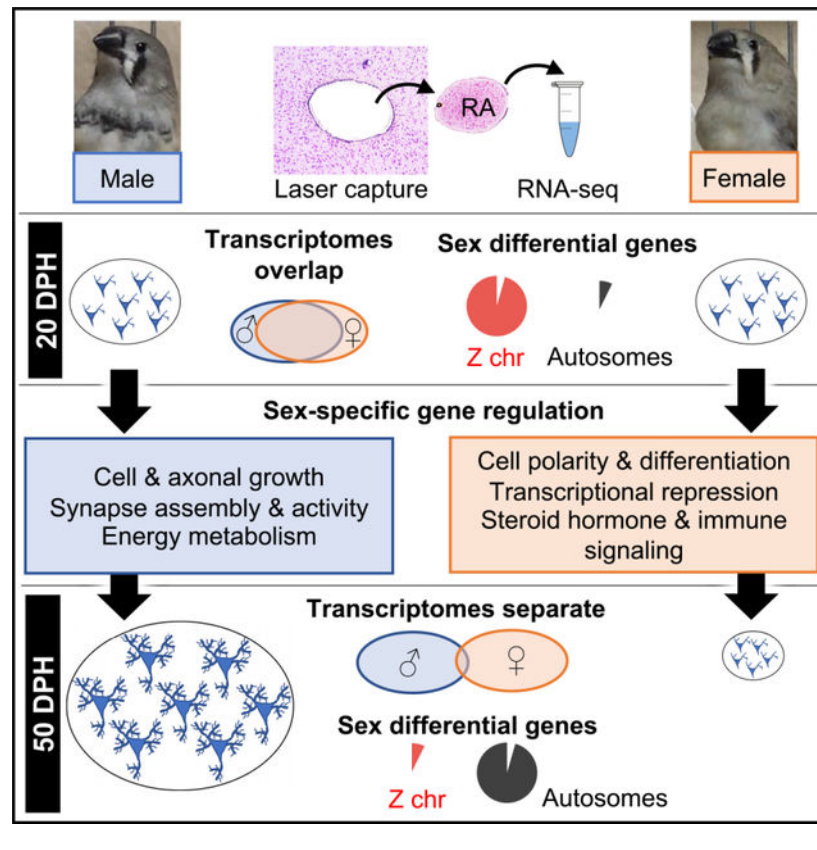
INTRODUCTION

Sex differences in neurodevelopmental processes give rise to lifelong sex differences in physiology, behavior, and health outcomes. Numerous brain sex differences have been reported that range in biological scale, but relatively few gross neuroanatomical sex differences have been documented thus far in vertebrates. A vast body of research has demonstrated the pivotal role sex steroid hormones play in sexual differentiation of neural tissue (Arnold and Gorski, 1984; Cooke et al., 1998). In contrast, much less is known about the roles of genetic sex differences, or about the transcriptome dynamics underlying the establishment of sex differences in the developing brain.

One of the most drastic known sexual dimorphisms in the brain is that of the song control regions in the zebra finch (*Taeniopygia guttata*), a songbird species in which only males sing (Zann, 1996). Zebra finches acquire their song through vocal imitation, a rare trait observed in only a small number of mammals (humans, cetaceans, pinnipeds, and possibly elephants and bats) and three groups of birds (songbirds, parrots, and hummingbirds) (Janik and Knörnschild, 2021; Jarvis, 2019). The brain system that drives song behavior is a network of

pallial, basal ganglia, and thalamic components (Figure 1A) comprising two interconnected circuits: the direct vocal-motor pathway, necessary for song production (Nottebohm et al., 1976, 1982), and the anterior pathway, necessary for song learning and adult song plasticity (Bottjer et al., 1984; Brainard and Doupe, 2002; Scharff and Nottebohm, 1991; Sohrabji et al., 1990). The robust nucleus of the arcopallium (RA), in particular, shows extreme sexual dimorphism in zebra finches (Figure 1B), being over five times larger in adult males compared with females (Nixdorf-Bergweiler, 1996). The RA is the main output nucleus of the telencephalic song system, and lesions of the RA severely disrupt song (Nottebohm et al., 1976). In the RA, signals from the anterior pathway converge with those of the direct vocal-motor pathway, and outputs are sent to brain-stem regions that innervate the avian vocal organ (syrinx) and coordinate respiration (Vicario, 1991). In terms of behavioral function, RA neurons are active during song production and are thought to encode the acoustic properties of song syllables (Hahnloser et al., 2002; Kimpo and Doupe, 1997; Leonardo and Fee, 2005; Yu and Margoliash, 1996).

The zebra finch RA undergoes major sex-specific morphological changes that overlap with the critical period for song learning. In contrast to the striking sexual dimorphism seen in adulthood, the RA appears monomorphic in young zebra finches (Figure S1A, top row). Over the first 3 weeks posthatch, the RA grows equally in volume in both sexes (Nixdorf-Bergweiler, 1996). Around 20 days posthatch (DPH), several days before males produce their first song-like vocalizations (i.e., subsong), the RA's growth trajectory begins to diverge; the male RA begins increasing in volume, and the female RA begins decreasing in volume. By 50 DPH, about the time when males are singing rudimentary, plastic song, the RA is already highly dimorphic (Figure S1A, bottom row) and approximates adult volumes (Nixdorf-Bergweiler, 1996). Over this 20–50 DPH window of development, sex-specific shifts in the RA's cytoarchitecture drive the observed volumetric growth in males and the regression in females. In males, the expanding volume of the RA is driven by increases in cell size and decreases in cell density, with no apparent change in total cell number (Bottjer et al., 1986). In contrast, the shrinking volume of the female RA is driven by the loss of neurons (Nordeen and Nordeen, 1988a), as well as a decrease in soma size (Konishi and Akutagawa, 1985). Due to these cellular changes, the adult male RA is characterized by more numerous, large, widely spaced cells, and the adult female RA is characterized by fewer, small, tightly packed cells (Figure 1B). In tandem with morphological dimorphism, the RA develops sex differences in innervation from afferents (Burek et al., 1994; Konishi and Akutagawa, 1985; Mooney and Rao, 1994; Nordeen and Nordeen, 1988a; Nordeen et al., 1992), cell survival (Kirn and DeVoogd, 1989), and excitability properties (Adret and Margoliash, 2002; Ölveczky et al., 2011; Zemel et al., 2021) (summarized in Figure 1C). In addition, developmental sex differences in expression levels have been characterized for several genes in the RA (Nevue et al., 2020; Tang and Wade, 2011; Wade et al., 2005; Wang et al., 2015b; Wild et al., 2001).

Considering the multifaceted and rapid nature of sex differentiation in the RA, we reasoned that many genes spanning a wide array of functional networks must be recruited to orchestrate sex-specific developmental programs. We also hypothesized that the RA's transcriptome would mirror its sexually dimorphic growth trajectory, in that male and female gene expression would look more similar at monomorphic stages than dimorphic

stages of development. To test these ideas, we characterized developmental changes and sex differences in the transcriptomic landscape of the RA. We used laser capture microdissection and bulk RNA sequencing (RNA-seq) to assay the male and female transcriptomes of the RA at the outset (20 DPH) and the peak (50 DPH) of its divergent growth trajectory (Nixdorf-Bergweiler, 1996). We show that the male and female RAs start out with similar transcriptomes, where sex differences in gene expression are mostly due to sex-linked genes, and then undergo two massively gene-rich and functionally distinct developmental programs.

RESULTS

Sex and age affect the RA's transcriptome

To characterize the transcriptome dynamics underlying the development of the drastic sexual dimorphism of the zebra finch song nucleus RA, we evaluated the effects of sex and age on the RA's genome-wide gene expression. We collected RA tissue from male and female juveniles (n = 5–7 per group) at 20 DPH, when the RA is monomorphic, and at 50 DPH, when the volume of the RA is over five times greater in males (Nixdorf-Bergweiler, 1996). We used laser capture microdissection to precisely extract the RA, from which we isolated high-quality total RNA for sequencing (see Figure S1B and STAR Methods for details). We found no evidence of sample outliers or batch effects based on hemisphere, RNA isolation batch, read depth, or sequencing lane. In total, we evaluated the expression levels for 21,955 zebra finch genes, of which 11,541 were associated with human orthologs in Ensembl.

To visualize the sample-to-sample variation and high-dimensional structure in our data, we performed a principal-component analysis (PCA) using the 500 genes with the highest variance across all samples. When plotting the first two principal components, which accounted respectively for 35% and 13% of the variance, the samples fell into three distinct clusters; the 20 DPH males and females intermixed within a single cluster, while the 50 DPH animals separated into male and female clusters (Figure 2A). Thus, when male and female RAs are mostly monomorphic (20 DPH), their transcriptome signatures closely resemble one another, and when male and female RAs have become dimorphic (50 DPH), the RA transcriptome signatures separate into sex-specific clusters. When all assessed genes (n = 21,955) were included, the 20 DPH groups remained clustered together, but could be bisected by a diagonal line through the cluster (Figure S2). In sum, the high-dimensional structure revealed by the PCA was in line with our hypothesis that the RA's transcriptome would parallel its morphological divergence.

Our statistical model detected significant effects (adjusted p < 0.01) of sex and age as main factors, and paired contrasts of specified groups (see group contrasts table in STAR Methods) yielded 3,394 developmentally regulated differentially expressed genes (DEGs) in males, 1,803 developmentally regulated DEGs in females, 339 sex-biased DEGs at 20 DPH, and 4,262 sex-biased DEGs at 50 DPH (Table S1). Among all these DEGS, 1,446 showed a sex + age interaction, i.e., their developmental trajectories were significantly sex dependent. Notably, many fewer genes were sex differential at 20 DPH relative to 50 DPH, consistent with our prediction that male and female RAs would show more similar gene expression profiles when the RA is monomorphic.

To validate the DEG analysis, we compared our results with published mRNA and protein expression patterns in the RA, focusing on the relative trends for each gene, and found consistent sex differences and developmental changes for SCN3B and SCN4B, which are associated with sex differences in key excitable properties of RA projection neurons (Zemel et al., 2021). We also found consistent sex differences and/or developmental changes for SCAMP1 (Tang and Wade, 2011), VIM (Tang and Wade, 2016), PVALB (Braun et al., 1991), ROBO1 and SLIT1 (Wang et al., 2015b), and GAP43/NEUM (Clayton et al., 2009). We also analyzed the subset of DEGs in male development that are known RA markers published in the Zebra Finch Expression Brain Atlas, ZEBrA (Lovell et al., 2020). Positive and negative RA markers show respectively higher and lower expression in the adult male RAs than in the surrounding arcopallium in the sagittal plane, such that the boundaries of the RA are clearly evident in the *in situ* hybridization pattern. Of the 73 RA markers that were DEGs in male development, 27 of 32 (84%) positive markers increased with age, and all 41 (100%) negative marker genes decreased with age (Table S2). Thus, the vast majority of developmentally regulated DEGs in males changed in the direction consistent with their adult male RA marker type. Assuming that most RA marker patterns emerge or intensify between 20 DPH and adulthood, this congruence provides further validation of the RNA-seq data.

Developmental changes in the RA's transcriptome are predominantly sex specific and more drastic in males

Massive shifts in the RA's transcriptome were apparent from the high number of developmentally regulated DEGs. Developmentally regulated DEGs were evenly distributed between directions of regulation (870 up- and 933 downregulated in females, and 1,686 up- and 1,709 downregulated in males); however, many more genes shifted their expression levels in males compared with females (Figure 2B). In addition, the absolute $\log_2$ fold changes of developmentally regulated DEGs were larger in males (1.06 mean; 0.78 median) than in females (0.87 mean; 0.63 median). These data strongly suggest that, compared with females, RA development in males recruits a broader gene network and undergoes more drastic shifts in expression level changes. Sex-specific developmentally regulated DEGs (n = 978 in females; n = 2,569 in males) outweighed shared ones (n = 825), further supporting the idea that the male and female RAs undergo distinct developmental programs. Interestingly, of the 825 DEGs that changed developmentally in both sexes, 760 (92%) changed in the same direction, and of these, only 70 were significant for an interaction between sex and age. Collectively, these findings provide evidence that sex-specific development of the RA is coordinated by largely nonoverlapping gene networks unique to each sex and suggest that shared developmental DEGs may be part of a sex-neutral developmental program.

Male-biased expression of Z-chromosome genes dominates early transcriptome sex differences in the RA

The majority of sex-biased DEGs at 20 DPH had positive $\log_2$ fold-change values, indicating greater expression in males than in females (Figure 2B, top left). Given that males are the homogametic (ZZ) sex, and that zebra finches lack global dosage compensation (Itoh et al., 2007, 2010), we suspected that many of these male-biased genes would be on the Z

chromosome. Indeed, 295 (87%) of the 339 DEGs from the 20 DPH sex contrast were on the Z, and all of them showed male-biased expression. In contrast, only 413 (10%) of the 4,262 DEGs from the 50 DPH sex contrast were on the Z, of which 388 (94%) were male biased. This overrepresentation of Z-linked DEGs at 20 DPH but not 50 DPH (Figure 3A) shows that sex differences in gene expression are dominated by sex chromosome genes early in RA development and then expand to thousands of autosomal genes as RA becomes sexually dimorphic. We note, however, that, while the Z-linked proportion of DEGs decreased with age, the total number of Z-linked DEGs increased. This indicates that additional Z-linked genes are coming into play as the RA becomes more dimorphic, and that sex-differential Z gene expression persists across this developmental window. Mirroring the sex-biased DEGs, sex expression ratios of all detectable genes across the genome showed a strong signal of male-biased expression from Z-linked genes at 20 DPH, but also evidence of developmental changes, namely large increases in the proportion and degree of sex-biased expression from autosomal genes at 50 DPH (Figure 3B). We interpret this as further evidence that sex differences in the RA's transcriptome are largely dominated by sex chromosome genes early on and then expand through the emergence of sex-differential autosomal gene expression as development progresses. This suggests, in turn, that early sex differences in RA gene expression may be primarily driven by sex differences in gene dosage, while those in later stages reflect more diverse mechanisms, for example, steroid hormones and other transcriptional regulators.

Because we aligned RNA-seq reads to a male zebra finch genome assembly, we could not evaluate W-chromosome-specific genes in that analysis. We did assess W-chromosome genes, however, by performing a detailed manual curation to better define its gene content in zebra finches. We found a large set of putative pseudoautosomal genes present on both the Z and the W chromosomes (n = 58; see W:Z pairs on Table S3), a subset of which were DEGs (n = 28). Interpretation of sex differences for these should be taken with caution, as some reads from female samples that did not align to the genome may relate to these W copies. Nonetheless, these DEGs represent only a small proportion of the Z-linked DEGs, and ultimately, the overwhelming male bias across Z-linked DEGs is entirely consistent with the lack of global dosage compensation in this species (Itoh et al., 2007, 2010). A very limited set of genes (n = 15) was found to be unique to the W (see W unique on Table S3), with few (n = 5) showing evidence of sex-differential expression based on public transcriptome data mapped to NCBI's RefSeqs (annotation release 106). *In situ* hybridization for LOC116806961, which encodes a novel protein with elements of possible retroviral-related origin, revealed very low to undetectable expression throughout the brain, including the RA. This gene did, however, show intriguing female-specific expression restricted to the lateral ventricle (Figure S3A), potentially within the proliferative zone (DeWulf and Bottjer, 2002, 2005), providing clear evidence of regional sex differences in brain expression of a W-specific gene in a bird. *In situ* assay for LOC116806962, a W paralog of the PIM1L family of kinases, replicated a broad brain distribution (Kong et al., 2010). Neither of the W-specific probes we tested showed evidence of sex-differential expression within the RA. Collectively, these findings suggest that W-specific genes play at most a limited role in the developmental sex differences of the RA transcriptome, although

further examination of W-specific gene expression within the RA is needed to settle this issue.

A hierarchical clustering analysis of all Z-linked genes appearing in at least one DEG set (n = 509) clustered most Z-linked DEGs (n = 431) into clusters 1–3 (Figure 3C), all higher in males and differing only in degree of developmental regulation. Only a small number of Z-linked DEGs were higher in females (i.e., cluster 5 in Figure 3C), showing developmental increases in females and/or decreases in males, which could reflect gene-specific dosage compensation. Gene ontology (GO) overrepresentation analysis (ORA) of these clusters identified one significant enrichment: protein lipidation (GO:0006497) in cluster 3. These clusters also contained DEGs with functions relevant to developmental processes. Among these, cathepsin L (CTSL; cluster 3) showed sex-specific developmental regulation, decreasing only in females, to become male biased at 50 DPH. We confirmed this pattern via *in situ* hybridization, which also revealed CTSL to be a strong positive RA marker in males (Figure 3D, left). The related cathepsin B (CTSB) was also developmentally regulated, increasing more in males than in females. CTSL and CTSB are both lysosomal cysteine proteases that have been linked to a wide array of functions in the brain, including extracellular matrix remodeling, neuropeptide synthesis, and apoptosis (Felbor et al., 2002; Funkelstein et al., 2010; Hook et al., 2012; Vidak et al., 2019). They may also play a role in synapse formation (Felbor et al., 2002; Stahl et al., 2007), and extracellular CTSL can directly stimulate axon growth *in vitro* (Tohda and Tohda, 2017). Assuming conserved function across vertebrates, the sex difference in CTSB/L could leave RA neurons more susceptible to lysosomally mediated apoptosis in females, while providing more neuroprotection and support for synapse organization and axon growth in males. In contrast, lipoprotein lipase (LPL; cluster 1), a discrete positive marker of the adult male RA (Figure S3B) that has been linked to lipid metabolism, neuronal differentiation, and neurite extension (Paradis et al., 2004), showed developmental increases in both sexes but was not significantly male biased at either age, a pattern supported by *in situ* hybridization (Figure 3D, right). Thus, some Z-linked genes show similar expression patterns across sexes, suggesting they may be linked to sex-neutral developmental processes in the RA.

Molecular pathways regulated during RA development are highly sex specific

To gain insight into the biological processes and molecular pathways of sex-differential RA development, we tested each DEG set for significantly enriched GO terms using both a competitive ORA and a noncompetitive gene set enrichment analysis (GSEA). We found substantial consensus between the results of the ORA and the GSEA, both revealing that GO enrichments for developmentally regulated DEG sets were quite different between sexes (summarized in Tables 1 and 2; all GO terms are reported in Tables S4 and S5). Significant themes unique to female development were related to hormones, cell polarity, cell movement inhibition, glial and oligodendrocyte differentiation, transcriptional regulation, and negative regulation of voltage-gated potassium channels. In addition, we observed female-specific enrichments related to immune signaling and RNA-mediated posttranscriptional gene silencing. These two enrichments are particularly intriguing in light of emerging evidence that neuroimmune signaling and microRNAs (miRNAs) may influence sex differentiation in the brain (McCarthy et al., 2015; Morgan and Bale, 2012). Of

the miRNAs that were DEGs, a few showed higher expression in males. Notably, MIR2954, a Z-linked gene unique to birds, showed male-biased expression at both 20 and 50 DPH. This miRNA shows considerable sex-biased expression across several tissues in the adult zebra finch, including the brain (Lin et al., 2014), and is regulated in response to song exposure, with a slight increase in males and decrease in females (Gunaratne et al., 2011). The other sex-biased miRNA was MIR9–1, which showed no sex difference at 20 DPH, but was significantly higher in males by 50 DPH. MIR9–1 is a variant of MIR9, which is known to regulate a suite of genes in the developing vertebrate brain, in turn affecting neuronal proliferation, migration, differentiation, and axon development (Radhakrishnan and Alwin Prem Anand, 2016). In contrast to female development, themes associated with DEGs in male development were related to cell morphogenesis and growth, development and maturation of axonal projections, metabolic and energetic processes, synapse organization and neurotransmission, and voltage-gated ion channel activity.

While the 20 DPH sex contrast was associated only weakly with a type I interferon pathway, many of the sex-specific developmental enrichments mentioned above also emerged for sex-biased DEGs at 50 DPH, including most of the GO themes for male development. In addition, the ORA results turned up several GO terms uniquely enriched in the 50 DPH sex contrast, including histone binding, transcription corepressor activity, transcription coregulator activity, response to monoamines, response to catecholamines, mRNA processing, cell-cell signaling involved in cardiac conduction, and cerebral cortex GABAergic interneuron differentiation. For these enrichments unique to the 50 DPH sex contrast, females expressed most of the associated genes at higher levels than males (Table S6). Finally, functional enrichments for the sex + age interaction DEGs contained many of the same themes as those for the paired contrasts; however, a few unique GO enrichments emerged, including β-catenin binding, insulin secretion, and insulin-like growth factor binding.

While it was possible that hundreds of sex-specific developmentally regulated DEGs would converge on similar functions, we did not find evidence of such convergence; not only were developmental DEGs mostly nonoverlapping between sexes, the related GO term enrichments were also highly sex specific. The fact that many GO themes associated with sex-specific development reappeared in the 50 DPH sex contrast and sex + age interaction results further supports the idea that major shifts in the RA's transcriptome reflect functional divergence between sexes. The paucity of significant enrichments for the 20 DPH sex contrast may reflect a true lack of functional sex differences at this age or, alternatively, may be due to fewer DEGs, human orthologs, or functional annotations for Z-linked genes.

Expression pattern clusters of sex + age interaction DEGs show distinct GO enrichments

Hierarchical clustering on all sex + age interaction DEGs (n = 1,446) identified nine clusters with unique developmental dynamics and sex differences (Figure 4A). When assessed by ORA (Table S7), the smaller clusters 4–9 did not yield significantly enriched terms, with the exception of chromatin binding and β-catenin binding for cluster 6. Clusters 1–3, in contrast, which together contained 1,006 (70%) of all sex + age interaction DEGs, were uniquely

enriched for different biological processes, demonstrating that directionally coordinated shifts in gene expression were associated with distinct functional networks.

Cluster 1 comprised 470 genes that became male-biased over development through an increase in males and/or a decrease in females, with GO enrichments being largely metabolic and mitochondrial processes. One example was solute carrier family 4 member 4 (SLC4A4), which codes for a sodium bicarbonate cotransporter and has been implicated in activity-dependent metabolic coordination between astrocytes and neurons (Ruminot et al., 2019). SLC4A4 was expressed at similar levels in 20 DPH RA and increased developmentally only in males, a pattern corroborated by *in situ* hybridization (Figure 4B, top right). This increase appears to be part of a large network of enriched cellular energetics pathways that evolves to support the energy demands of large male RA neurons (Adret and Margoliash, 2002). While not part of a significant enrichment set, cluster 1 also encompassed genes linked to growth and development. Pleiotrophin (PTN), for example, encodes a secreted cytokine required for dendrite development in newborn hippocampal neurons (Tang et al., 2019) and implicated in neuronal differentiation, axon growth, and synapse formation (González-Castillo et al., 2015). PTN was developmentally regulated in a sex-dependent manner; it was similarly expressed in males and females at 20 DPH, but became a strikingly male-specific positive marker of the RA at 50 DPH (Figure 4B, bottom left). The diffuse signal distribution among darkly stained cell bodies suggests PTN mRNA may be present in neurites, where it could act locally in supporting the growth of axons or dendrites, potentially contributing to the greater dendritic arborization of RA neurons in males compared with females (Gurney, 1981).

Cluster 2 contained 260 genes that became female biased over development through marked decreases in males and showed GO term enrichment related to axon development, synapse assembly and organization, neurotransmission, and voltage-gated potassium channels. A striking example was the gene that encodes stathmin 1 (STMN1), a cytosolic phosphoprotein that destabilizes microtubules (Curmi et al., 1999). Downregulation of STMN1 is necessary for normal dendritic arborization in cerebellar Purkinje cells (Ohkawa et al., 2007) and axon formation in hippocampal cells (Watabe-Uchida et al., 2006). The *in situ* pattern (Figure 4B, top left) confirmed high expression within the RA at 20 DPH in both sexes and persistent high expression in females at 50 DPH, but substantially decreased expression in males at 50 DPH. This developmental trend appears to continue, as STMN1 is an exquisitely high-contrast negative marker of the adult RA (Lovell et al., 2020). Given the neuromorphogenic effects of STMN1 suppression in mammalian neurons, downregulation of STMN1 in the male RA may encourage the elaboration of axons and/or dendrites.

Cluster 3 genes became female biased through increases in females and/or decreases in males and were associated with GO terms like negative chemotaxis, voltage-gated ion channels, transcription cofactor binding, and synapse organization. Chemotaxis is a key part of neural circuit development that involves directing the growth of cells and neurites through both attractive and repellent factors (Dickson, 2002; Song and Poo, 2001). Notably, five of six cluster 3 DEGs associated with negative chemotaxis (SEMA3F, SLIT1, NRG3, FLRT2, and SEMA4D) decreased over development in males only, and one (SEMA5A) increased in females only. This sex-specific regulation of chemorepulsive cues provides

a potential channel through which sex differences in RA afferents may be established. Likewise, 15 of 20 (75%) of the subset of cluster 3 DEGs linked to synapse organization exhibited developmental decreases in males, but no developmental regulation in females. Combined with the predominance of synapse and axon development-related enrichments in male but not female development, these findings suggest that genes involved in orchestrating connectivity are more widely regulated in males. Cluster 3 also showed enrichment for voltage-gated calcium channels, including several α1 subunits (CACNA1H, CACNA1D, CACNA1B, and CACNA1I). Calcium voltage-gated channel subunit α1 E (CACNA1E), another α1 subunit and a known negative marker of the adult male RA (Friedrich et al., 2019), was in cluster 6, whose overall pattern closely resembled that of cluster 3 (Figure 4A). CACNA1E showed similar expression between males and females at 20 DPH but was selectively downregulated in the RA over male development (Figure 4B, bottom right). CACNA1E codes for an R-type voltage-gated calcium channel that limits depolarization in mammalian hippocampus (Bloodgood and Sabatini, 2007; Wang et al., 2015a). This raises the possibility that developmental downregulation of CACNA1E in males contributes to the male-specific increases in action potential amplitude observed in developing RA neurons (Zemel et al., 2021).

Sex differences in specific gene families

Based on the RA's multifaceted dimorphic development, we hypothesized that several key gene families and functional themes related to regulation of transcription, cell growth, and apoptosis would show developmental changes and/or sex differences in the RA, as well as genes related to sex steroid hormones and intrinsic neuronal excitability. While there were indications of these gene families in the GO analysis results, more directed term-based searches of the zebra finch gene descriptions revealed substantial sets of related sex-biased and developmental DEGs (Table S8). For instance, consistent with volumetric growth of the male RA, many growth factor genes showed male bias, including FGF2, which has been shown to reduce pyknosis in the female RA when administered exogenously (Nordeen et al., 1998). Males also expressed higher levels of NTRK2, a BDNF receptor, consistent with previous reports implicating the BDNF signaling pathway in sexually dimorphic song system development (Akutagawa and Konishi, 1998; Chen et al., 2005; Dittrich et al., 1999; Johnson et al., 1997). Importantly, several genes that promote apoptosis showed female bias (e.g., EVA1A, AATK, ANKDD1A), while in contrast, genes that suppress apoptosis showed male bias (e.g., CFLAR, DDIAS, NIBAN1). In line with a role for sex steroids in song system masculinization, males expressed higher levels of genes encoding sex steroid metabolism and biosynthesis enzymes (e.g., HSD17B4, HSDL2, SRD5A2). Many voltage-gated ion channel genes were female biased at 50 DPH, largely due to developmental decreases in males; however, some genes exhibited large male-specific developmental increases, including SCN4B, which is associated with the developmental emergence of large sex differences in resurgent sodium current and spiking rates of RA projection neurons (Zemel et al., 2021).

Almost 200 DEGs were found to encode transcription factors (TFs), including genes with some of the largest male-biased fold changes in this dataset (e.g., SIX2 and NKX2–8). Notably, this included TFs on the Z chromosome with male-biased expression at 20 DPH

(BDP1, BTF3, GTF2H2, and RFX3), representing candidate sex-linked TFs that might be exerting broad regulatory actions at this early age. As a follow-up, for each of the paired contrast DEG sets, we examined whether the TF binding sites (TFBSs) for DEGs that encode TFs showed enrichments in the promoters of the corresponding DEG set. We found significant TFBS enrichments in the DEG sets for male and female development (Figure 5A, left and middle), but the largest set of enriched TFBSs was seen in the 50 DPH sex contrast (Figure 5A, right). The majority of these were from DEG TFs that showed female-biased expression, most of which have been associated with pro-apoptotic function (Table S9). One notable example was KLF11, whose TFBS was enriched in all three DEG sets (Figures 5A, S4A, and S4B); thus, KLF11 may regulate extensive gene networks that control key processes like cell death in RA development. The enriched TFBSs from male-biased DEG TFs were mostly linked to anti-apoptosis or anti-hypoxia protection. These findings solidify apoptosis as a major pathway regulated in concert with the emergence of the RA's sex dimorphism, and point to specific transcriptional networks that regulate cell survival and death. Analysis of non-DEG TFs, which were a larger set than DEG TFs, also showed evidence of TFBS enrichment in the promoters of DEG sets (Figure S4C). Enriched TFBSs from non-DEG TFs were mostly overlapping across all DEG sets (not shown) rather than specific to a given comparison, suggesting they may relate to broad developmental processes. Furthermore, the fact that these enriched TFBSs are from non-DEG TFs suggests they are not directly mediating the emergence of sex differences in the RA's transcriptome in the period examined here. Of course, it is possible these TFs are sex-differentially expressed prior to 20 DPH, or that they influence expression indirectly by interacting with DEG TFs.

Consistent with previous studies reporting a lack of expression and no sex or developmental differences in estrogen receptor mRNA within the RA (Gahr, 1996; Jacobs et al., 1999), the estrogen receptor genes ESR1 and ESR2 had relatively low abundance and were nondifferential across all comparisons. Furthermore, there was no evidence of TFBS enrichment for ESRs in the analysis of non-DEG TFs (Figure S4C). Androgen receptor (AR) was also somewhat low in abundance but showed an intriguing increase in females (Figure S5). We were unable to confirm this finding, as the AR transcript is undetectable by our standard *in situ* protocol, requiring a radioactive approach (Kim et al., 2004). AR was included in the TFBS enrichment analysis for DEG TFs, but no enrichment was found for its binding site in DEGs (Figure 5A). The lists of DEGs containing TFBSs for AR and ESR1 in their promoters are provided in Table S9.

DISCUSSION

Understanding how sex differences in the brain manifest requires that we understand the molecular factors orchestrating their development. Using RNA-seq to assay gene expression during a window of neural sex differentiation, we observed large-scale sex differences and developmental shifts in the transcriptome of the sexually dimorphic nucleus RA. Previous studies have assessed developmentally regulated genes in the male RA (Clayton, 1997; Mori and Wada, 2015; Velho et al., 2007; Wada et al., 2006) and HVC (Mori and Wada, 2015; Shi et al., 2021), and one recent study reported sex differences in song nuclei transcriptomes of 30 DPH zebra finches treated with an estrogen synthesis inhibitor (Choe et al., 2021). While

providing some insight into genes involved in the hormone sensitivity and masculinization of song nuclei, these studies either assessed developmental changes only in male song nuclei that are already sexually dimorphic or examined a single age, and thus did not address developmental dynamics in gene expression. By evaluating the combined effects of sex and age on the RA's transcriptome, our study provides novel insights into how gene expression changes in a sex-dependent manner during sexually dimorphic brain development.

Previous high-throughput studies comparing male and female gene expression in developing brains generally found fewer sex differences than our study; however, they assayed larger and more heterogeneous brain areas (Diddens et al., 2021; Tomaszycki et al., 2009; Wada et al., 2006). While some of these studies used follow-up histochemical methods to assay expression in specific brain nuclei, our approach of quantifying gene expression directly from microdissected tissue is more efficient and sensitive in detecting differential genes. In addition, the RA's discreteness combined with direct laser capture from Nissl-stained sections allowed for extremely precise extraction of RA cells. Crucially, our study was also designed to minimize several confounds that have an impact on gene expression, yet are often not adequately addressed, including behavioral state, circadian rhythms, age variability, and genetic relatedness.

We found evidence that wide-ranging, sex-specific gene networks are associated with sexually dimorphic developmental pathways. In line with our initial hypothesis that developmental changes in the RA's transcriptome would mirror the RA's sexually dimorphic growth trajectory, the transcriptional landscape of the RA indeed followed its morphological sex divergence. Fewer than 400 genes were sex biased at 20 DPH, whereas over 4,000 genes were sex biased at 50 DPH—more than a 10-fold increase over this pivotal developmental window. We also identified age-dependent contributions of autosomal versus sex chromosome genes to these genome-wide sex differences; Z-linked genes made up the vast majority of sex-biased genes at 20 DPH but not 50 DPH, consistent with the notion that early sex bias in sex chromosome gene expression might affect subsequent sexual differentiation (Arnold, 2009).

Our study puts forth solid evidence that the RA undergoes two distinct, sex-specific developmental programs carried out by largely nonoverlapping gene networks. For one, most developmentally regulated genes were specific to one sex. The majority of DEGs that were common to both male and female development tended to change in the same direction and to a similar extent, suggesting these genes may be involved in basal developmental processes necessary for both sexes. Furthermore, we did not find evidence of functional convergence, as RA development was characterized by highly sex-specific GO term enrichments, with little to no overlap between sexes. The developmental program in males appears to recruit networks involved in cellular energetics, cell morphogenesis and growth, axon formation and myelination, cell excitability, and multiple synaptic processes, including assembly, organization, and neurotransmission. In contrast, female development seems to be linked to hormone and immune signaling, negative regulation of cellular movement, cell polarity, glial cell differentiation, and various mechanisms of gene silencing. Focused examination of specific gene families and functions revealed developmental and sex-biased regulation of many genes encoding growth factors, apoptosis regulators, sex

steroid enzymes, voltage-gated ion channels, and TFs. A subset of TFs showed binding site enrichment within their corresponding DEG sets, suggesting their role in modulating broad developmental gene networks. These findings identify molecular players and pathways that differentiate the male from the female RA, and that may serve as the molecular substrate of RA sexual dimorphism. This includes some genes (e.g., BDNF) and pathways (e.g., apoptosis, cell growth, synapse formation) previously linked to neural sexual dimorphism (Akutagawa and Konishi, 1998; Chen et al., 2005; Dittrich et al., 1999; Johnson et al., 1997; Mccarthy et al., 2017), but we also identified numerous novel sex differences in gene expression whose mechanistic link to sex-specific development has yet to be established.

A common feature of sexually dimorphic brain regions, including the RA, is sensitivity to sex steroid hormones, particularly estrogen (reviewed in Wade and Arnold, 2004). Most notably, the administration of estradiol to young female zebra finches prompts the development of masculinized song nuclei and singing in the female zebra finches (Adkins-Regan and Ascenzi, 1987; Adkins-Regan et al., 1994; Gurney, 1982; Gurney and Konishi, 1980; Pohl-Apel and Sossinka, 1984; Simpson and Vicario, 1991a, 1991b). However, sex steroids alone are insufficient to fully determine sex differences in the song system. For one, estrogen-induced masculinization of females is partial (Adkins-Regan et al., 1994; Gurney, 1982; Gurney and Konishi, 1980; Simpson and Vicario, 1991b), and efforts to block masculinization of the male song system by inhibiting estrogen signaling produce only modest effects (Ball et al., 1994; Choe et al., 2021; Merten and Stocker-Buschina, 1995; Wade et al., 1999). Most tellingly, in a gynandromorph zebra finch that was genetically male on one side of its body and female on the other, song nuclei, including the RA, were smaller on the genetically female side, demonstrating the insufficiency of circulating hormones to fully masculinize the song system (Agate et al., 2003). Recent work suggests that early RA gene expression may be largely unaffected by estrogen manipulation (Choe et al., 2021), and in line with previous studies (Gahr, 1996; Jacobs et al., 1999), we found no evidence that estrogen receptor gene expression was sex biased or developmentally regulated. Taken together, these results imply that brain sex differences are in part determined by hormone-independent and cell-autonomous mechanisms. One such potential mechanism is differential expression of sex-linked genes. In our study, sex-biased genes at 20 DPH were overwhelmingly Z linked. In addition to identifying the specific set of Z-chromosome genes that are differential in the RA at the outset of its divergent growth trajectory, our findings show that sex differences in Z-linked gene expression precede the development of gross morphological sex differences. This is consistent with the hypothesis that differences in sex chromosome gene expression may affect early developmental processes associated with the RA's sexually dimorphic transformation. We note, however, the possibility that the transcriptome sex differences we detected at 20 DPH may be unrelated to the sexually dimorphic development of RA. Alternatively, they might reflect sex differences in RA cell type composition, such as greater numbers of nonneuronal cells in males (Nordeen and Nordeen, 1996) or perhaps other nuanced sex differences yet to be described for RA.

We must also consider extrinsic factors that could initiate sexual dimorphism in the RA; in particular, the presynaptic influences from the RA afferents HVC and LMAN. Around 30–35 DPH, the RA is innervated by the premotor song nucleus HVC (Burek et al., 1994; Konishi and Akutagawa, 1985; Nordeen and Nordeen, 1988b). The HVC is commonly

described as present only in males, but tract tracing (Gurney, 1981; Shaughnessy et al., 2019) and optical imaging of neural activity (Wang et al., 1999) suggest that this projection also forms in females, although probably less robustly, if only because the HVC has many fewer cells in females than in males (Burek et al., 1994; Konishi and Akutagawa, 1985; Nordeen and Nordeen, 1988b). Early HVC lesions block subsequent increases in volume and soma size in the male RA (Akutagawa and Konishi, 1994) and prevent estrogen-induced masculinization of the female RA (Herrmann and Arnold, 1991), consistent with a major role of HVC afferents in RA masculinization. In contrast, the LMAN-to-RA projection is comparable between the sexes around 20 DPH, but undergoes a gradual loss of neurons in females that ultimately results in a weaker projection compared with males (Nordeen et al., 1992). Early lesions of the male LMAN block subsequent increases in RA volume and cell number (Akutagawa and Konishi, 1994; Johnson and Bottjer, 1994), and there is evidence that neurotrophins transported from the LMAN modulate cell survival in the RA (Johnson et al., 1997). Based on the known influences and transformation of both these projections during the age window we examined, we reason that some of the gene regulation we observed in the RA may result from developmental changes and sex differences in these major RA inputs. For example, these afferents could modulate expression of key cell survival or growth genes in the RA in a sex-dependent manner.

We acknowledge that not all genes and pathways identified in this study necessarily contribute directly to sexually dimorphic properties in the RA, and some sex-biased genes may actually serve to prevent sex differences (de Vries, 2004); thus, further experimentation is required to evaluate candidate genes. Moreover, given the RA's cytoarchitectural changes (e.g., cell size, number, and density) during development, bulk RNA-seq data limit our ability to draw conclusions about expression per cell or cell type. Nonetheless, marked sex differences in developmental gene expression are a prominent feature of the RA, and several enrichments identified in our GO term analyses suggest cell-type-specific processes. For example, the observation that glial cell differentiation was enriched in female development is intriguing, considering that early sex differences in nonneuronal RA cells have been hypothesized to contribute to sexual differentiation of the RA (Nordeen and Nordeen, 1996). We also note that adult transcriptome sex differences, including some Z-linked genes, have been described in the premotor song nucleus HVC of other songbird species, regardless of sex differences in singing (Ko et al., 2021). Therefore, an open question for future studies is whether the developmental sex differences in the RA's transcriptome described here relate to sex differences in zebra finch singing.

In sum, while little is known about the ontogeny of sexual brain dimorphism in any species, our study clearly illustrates how the emergence of the RA's dimorphism is associated with massive, sex-specific shifts in the RA's molecular landscape that point to unique, active processes underlying both male growth and female regression. The sheer extent of the transcriptome sex differences we detected vastly exceeds those of previous studies that analyzed larger areas or whole brains. While this difference may be partially due to methodological advantages conferred by unique cytoarchitectonic features of avian brains, and/or the robustness of the RA's dimorphism, it raises the salient possibility that averaging gene expression levels across broad brain areas could mask or minimize sex differences that become apparent only when comparing more discrete brain regions or cell populations.

In line with this, we note that the sex-biased expression ratios we detected (both for the Z-linked and for the autosomal genes) are considerably higher than those previously seen using whole-brain samples on microarrays (Itoh et al., 2007). Importantly, our finding that early sex-biased gene expression is predominated by sex chromosome genes supports the growing evidence that sex-linked genes contribute to sexual differentiation of the brain, and to the emergence of a major brain dimorphism. Last, our results suggest the involvement of noncanonical pathways, significantly expanding the realm of potential targets and drivers of brain sex differences for future studies.

Limitations of the study

While providing extensive data on the development of transcriptome sex differences in one of the most dimorphic brain nuclei known, the present study does not address possible sex differences in specific cell types in the RA, a question that requires single-cell/nucleus sequencing. In addition, we have identified numerous candidate genes that may play a role in the sexually dimorphic differentiation of the nucleus RA, but establishing causal links will require gene manipulation approaches. Last, our study focused on morphological changes, so we have not examined possible links between the identified molecular sex differences and the emergence of sex differences in singing behavior.

STAR★METHODS

RESOURCE AVAILABILITY

Lead contact—Further information and requests for resources and reagents should be directed to and will be fulfilled by the lead contact, Claudio V. Mello (melloc@ohsu.edu).

Materials availability—This study did not generate new unique reagents. All plasmids used for *in situ* hybridization are part of the zebra finch brain cDNA ESTIMA collection, previously described in Replogle et al. (2008), and are available upon request in the Mello lab.

Data and code availability—All RNA-seq data generated in this study have been deposited at NCBI's GEO (GEO: GSE191296) and are publicly available as of the date of publication. All code and custom functions used for RNA-seq analyses were written in R using RStudio and various Bioconductor packages, and are available online (Friedrich, 2022). Codes used for transcription factor analysis were written in Python and are available online (Andrade and Velho, 2022a; 2022b). Any additional information required to reanalyze the data reported in this paper is available from the lead contact upon request.

EXPERIMENTAL MODEL AND SUBJECT DETAILS

Zebra finches (Taeniopygia guttata, castanotis)—All procedures involving live birds were approved by the OHSU Institutional Animal Care and Use Committee, and are in accordance with NIH guidelines. All juveniles (used for RNAseq and *in situ* hybridization analyses) and most adults (used for *in situs* only) were obtained from our breeding colony; some additional adults used for *in situ* hybridization only were purchased from a commercial supplier (Magnolia Bird Farm). All birds were kept under a 12:12 light/dark cycle and

supplied daily with seed, millet spray, water, egg food, cuttlebone, soluble grit, and kale ad libitum. Juveniles were raised by both parents in single family breeding cages, where they remained until the target day post-hatch (20 or 50 DPH) was reached. Captive zebra finch clutches often hatch over a period of several days, so to minimize age variability within groups, we devised a method to track the exact age of each juvenile. We used nontoxic food coloring to dye down feather patches in distinctive patterns (e.g. red head, green flanks) on hatch day, then transitioned to leg banding around 10 DPH. Sex was determined around 10 DPH using a PCR protocol (see PCR sexing in Method details), and later confirmed postmortem by gonad inspection. From a total of 21 juveniles (5 males exactly 20 DPH, 5 females exactly 20 DPH, 6 females 47–50 DPH, and 5 males 46–50 DPH), we generated a total of 22 samples for RNA-seq as one 50 DPH female gave rise to two samples, one from each hemisphere. Sex was integral to our experimental design, therefore individuals of both sexes were included, and interaction effects between sex and age were examined as part of the statistical analysis. To minimize relatedness as a confound, the 21 juveniles born of 11 different breeding pairs were assigned pseudorandomly to groups such that siblings would not be contrasted against each other in paired comparisons (see group contrasts table below), i.e., we paired a 20 DPH male and a 50 DPH sibling female, or a 20 DPH female and a 50 DPH sibling male. For *in situ* hybridizations, an additional set of 12 total juveniles, aged 20 DPH (3 males and 3 females) and 50 DPH (3 males and 3 females), were obtained from our breeding colony and euthanized within ± 2 days of the target age.

Group contrasts table

Result set name	Groups contrasted	DEG type
Female development	20 DPH females vs 50 DPH females	Developmentally regulated in females
Male development	20 DPH males vs 50 DPH males	Developmentally regulated in males
20 DPH sex contrast	20 DPH females vs 20 DPH males	Sex-biased
50 DPH sex contrast	50 DPH females vs 50 DPH males	Sex-biased
Sex + age interaction	All four groups	Developmentally regulated in a sex-dependent manner

METHOD DETAILS

PCR sexing—The sex of juvenile birds was determined using the PCR sexing protocol described by Soderstrom et al. (2007). This protocol utilizes two sets of primers that uniquely target the gametologs of the CHD gene on the Z and W chromosomes, producing a W-specific fragment of 179 bp and a Z-specific fragment of 242 bp. Blood samples were collected from live juveniles around 10 DPH. After cleaning the area with an ethanol wipe, a sterile 30 gauge needle was used to gently lance the blood vessel immediately distal to the bird's knee. A small droplet of blood was absorbed onto a sterile piece of filter paper that was then placed into a microcentrifuge tube. To suspend the blood, 1 mL of distilled water was added to each sample tube and mixed via inversion. Samples were allowed to rest at room temperature for 30 min before being centrifuged at $15,000 \times g$ for 3 min. The supernatant was carefully extracted and discarded, leaving behind a small volume of collected blood cells and the filter paper. To each of these sample tubes, 200 μL of a 5% suspension of Chelex 100 (Bio-Rad Laboratories) in distilled water was added. The tubes

were incubated for 30 min at 56°C, vigorously vortexed for 10 s, and suspended in boiling water for 8 min. After boiling, samples were vortexed again for 10 s, then centrifuged for 3 min at 15,000 × g to sequester Chelex beads at the bottom of the tube. From each tube, 2.5 μL of supernatant was extracted and used as template in a 25 μL PCR reaction that also contained: 10X PCR Reaction Buffer (Invitrogen), 50 mM MgCl$_2$ (Invitrogen), 10 mM dNTP mix (Invitrogen), 10 μM W-Forward primer GGGTTTTGACTGACTAACTGATT, 10 μM W-Reverse primer GTTCAAAGCTACATGAATAAACA, 10 μM Z-Forward primer GTGTAGTCCGCTGCTTTTGG, 10 μM Z-Reverse primer GTTCGTGGTCTTCCACGTTT, 1 unit Platinum Taq DNA polymerase (Invitrogen), and nuclease-free water. The reaction was run for 30 cycles on a thermocycler: 94°C for 30 s, 56°C for 45 s, and 72°C for 45 s. Finally, 5 μL of amplified PCR product mixed with 2 μL loading dye was run on a 2% agarose gel to assess band patterns.

Animals and tissue preparation—Upon reaching the target age, juveniles intended for RNA-Seq experiments were removed from their home cage and quickly euthanized by decapitation. To minimize the acute effects of variability on behavioral (e.g., singing), sensory (e.g., hearing song), and social states (e.g. isolation), which are known to induce changes in brain gene expression (Dong et al., 2009; George et al., 2019; Gunaratne et al., 2011; Mello et al., 1992; Whitney et al., 2014), as well as minimize circadian effects, juveniles were euthanized within 20 min of lights-on, and no singing was observed for any juvenile in this time window. The additional set of 12 juveniles used for *in situ* hybridizations were also obtained from our breeding colony, noting that these birds were collected at various times during the day. All brains were rapidly dissected into hemispheres, placed in a plastic mold, covered in chilled TissueTek OCT (Sakura Finetek USA, Inc.; Torrance, CA), and flash frozen by placing molds into a slurry of pulverized dry ice and isopropanol. Once frozen, brains were transferred to a −80°C freezer for storage until cryosectioning.

***In situ* hybridization—**We performed *in situ* hybridization on RA sections from juvenile male and female brains (n = 3–4 per sex per age) to provide independent validation of the RNA-seq data, as well as to characterize the expression patterns of select DEGs in more detail, including their expression in the arcopallium outside RA. Typically, each probe was minimally hybridized to brain sections from a test bird and from one bird from each age and sex group. In a few cases we also performed *in situ* hybridization on brain sections from an adult male. When choosing genes for *in situ* hybridization, we looked for DEGs that a) showed high absolute log$_2$ fold changes in relevant contrasts, b) were located on chromosome Z or W, c) were representative of an expression pattern cluster, d) had functional annotations of interest, or some combination thereof.

Digoxigenin (DIG)-labeled riboprobe synthesis and *in situ* hybridization was performed as described in Carleton et al. (2014). Briefly, cDNA clones from the ESTIMA collection (Replogle et al., 2008) were selected based on their alignment to and specificity for the target locus (Lovell et al., 2020). Clones were grown overnight in LB medium supplemented with 1% ampicillin. Plasmids were isolated with a QIAprep Spin Miniprep Kit (Qiagen), digested with BssHII (NEB) to release the cDNA insert, and purified using a QIAquick

PCR purification kit (Qiagen). We used 2 μg of template DNA for reverse transcription to generate antisense riboprobes. Riboprobes were synthesized using T3 RNA polymerase (Promega) and DIG RNA labeling mix (Roche). Riboprobes were then purified using a Sephadex G-50 column and stored at −80°C until use.

Brains were sectioned at 10 μm on a Leica CM1850 cryostat and mounted onto charged microscope slides. Prior to hybridization, slides were briefly fixed for 5 min at room temperature in 3% paraformaldehyde and acetylated for 10 min in a solution containing 1.35% triethanolamine and 0.25% acetic anhydride. For each gene hybridized, efforts were made to reduce experimental variability including fixing, acetylating, and hybridizing all slides at the same time with the same batch of solutions. Slides were hybridized overnight at 65°C in a hybridization solution consisting of 50% formamide, 2X SSPE, 2 μg/μL tRNA, 1 μg/μL BSA, 1 μg/μL polyA, and 2 μL DIG-labeled riboprobe in DEPC-treated H2O. The next day, slides were washed in 50% formamide 2X SSPE solution followed by two 30 min washes in 0.1X SSPE at 65°C, agitated every 10 min. Following the high stringency washes, the sections were briefly permeabilized in TNT (100 mM Tris–HCl pH 7.4, 150 mM NaCl, 0.3% Triton X-100) and blocked in TNB (100 mM Tris–HCl pH 7.4, 150 mM NaCl, 0.36% w/v BSA, 1% skim milk) for 30 min in a humidified chamber at room temperature. Slides were then incubated in an alkaline phosphatase conjugated anti-DIG antibody (Roche, 1:600) in TNB for 2 h in a humidified chamber at room temperature. Slides were then washed twice for 15 min in TMN (100 mM Tris–HCl, 150 mM NaCl, 5 mM MgCl2) and developed for 1–3 days in filtered BCIP/NBT Substrate Solution (PerkinElmer) at room temperature.

Laser capture microdissection—Several precautions were taken to limit RNA degradation by ribonucleases (RNases), including the use of RNase-free materials, cleaning equipment and work areas with RNase Away (Molecular BioProducts), and frequently changing gloves and staining solutions. Frozen brains were taken from the −80°C freezer, allowed to equilibrate to ~ −18–20°C in the cryochamber for 30 min, and sectioned on a Leica CM1850 cryostat at 12 μm thickness. As sectioning advanced through the brain, Nissl staining of parasagittal sections mounted on regular glass slides was used to assess brain anatomy until the medial edge of RA was visible. PEN membrane glass slides (Leica, No. 11505158) were labeled then UV treated for 15 min on a TFX-20M transilluminator (Life Technologies). Brain sections containing RA were mounted onto UV-treated PEN slides, with the exception of every 12th or 16th section, which was mounted on a frosted glass slide and Nissl stained to assess the level of RA. To avoid freeze-thaw cycles between the successive mounting of multiple sections onto each slide, four sections at a time were cut and arranged on the cryostage using RNase-free paint-brushes, then mounted simultaneously onto a room temperature PEN slide. As soon as sections had fully adhered, slides were transferred to 50 mL Falcon tubes containing chilled 100% ethanol and stored within the cryostat. Sectioning continued until the extent of RA was collected. Slides were then stained at room temperature, one at a time, using a series of ethanolic solutions prepared from RNase-free ethanol, cresyl violet acetate, and NanoPure water in 50 mL Falcon tubes to minimize hydration-activated RNase activity during staining. Specifically, slides were immersed for 30 s in each the following: 100% ethanol, 95% ethanol, 75% ethanol, 4%

cresyl violet in 75% ethanol, 75% ethanol, 95% ethanol, 100% ethanol, and again in 100% ethanol. Ethanol series solutions were changed out every 4–6 slides, and the cresyl violet staining solution was pipetted onto each slide to avoid contaminating the stock.

Laser capture microdissection was performed immediately after staining on a Leica LMD 6500. The surrounding work area and equipment were wiped down with RNase Away (Thermo Scientific) before beginning laser capture each day. Tissue was collected into 0.5 mL microcentrifuge tube caps containing 40–70 μL of RLT buffer (Qiagen) spiked with 10 μL of β-mercaptoethanol per 1 mL of buffer. The laser path around RA was conservatively drawn around the core of RA, excluding the surrounding cells with elongated morphology, and we confirmed successful capture by inspecting collection tube caps (Figure S1B). Once laser capture for 2–4 slides was complete, collection tubes were carefully closed and removed from the collection device, vortexed for 30 s, then immediately placed on dry ice. To minimize RNA degradation, this procedure was repeated in batches of 2–4 slides until the whole of RA was captured, then collection tubes were transferred to a −80°C freezer until RNA isolation. All RA tissue was microdissected and immersed in RNA-stabilizing solution within 1 h after staining.

RNA isolation and RNA-seq—Sample tubes were thawed in a gloved hand until no particulate was visible in the solution, then vortexed for 30 s. RNA was isolated using the RNeasy Micro Kit (Qiagen) with on-column DNase digestion. RNA isolation was performed in randomized batches of 4–5 samples and according to kit instructions with two exceptions: 1) an additional 80% ethanol column wash was performed immediately after the first, and 2) the RNase-free water used to elute the RNA was incubated on the column for 10 min prior to centrifuging to increase RNA yield. Isolated RNA samples were stored at −80°C until submission to the OHSU Massively Parallel Sequencing Shared Resource. We opted not to pool samples, and thus retained information about individual sample variability while maximizing statistical power. RNA quality was assessed on a Bioanalyzer 2100 using the high sensitivity RNA 6000 Pico Kit (Agilent). The median RIN for all samples was 8.6, and all but one sample (RIN = 6) had a RIN exceeding 7. cDNA libraries were generated using the SmartSeq v4 PLUS kit (Takara Bio USA). Paired end sequencing (2×100 bp) was performed on the NovaSeq 6000 S4 flow cell (Illumina) to a target depth of 50 M reads per sample.

Quality control and trimming were performed prior to genome alignment using trimmomatic (v0.36) (Bolger et al., 2014), and no issues were detected from FastQC (v0.11.9) (Andrews, 2010) reports. Splice-aware STAR (v2.6.1) (Dobin et al., 2013) was used to align reads and generate read counts per gene based on the bTaeGut1_v1.p zebra finch assembly (GCF_003957565.1) and associated genome features from the NCBI *Taeniopygia guttata* Annotation Release 104. At the time of this analysis, this was the best annotated zebra finch genome assembly in NCBI.

Curation of zebra finch W chromosome genes—To curate zebra finch W chromosome genes (Table S3), we first retrieved the full list of chromosome W genes from the zebra finch genome (all chromosome W RefSeqs from bTaeGut1.4.pri). We note that while bTaeGut1.4.pri derives from a male, it artificially includes the W chromosome,

which is derived from a previous female assembly (bTaeGut2.pat.W.v2). We then identified all W genes annotated with a gene symbol or description, and sorted those with annotated copies on both the W and Z chromosomes from those with an annotated copy on the W only. Next, for unannotated W chromosome genes (with LOC annotations and/or ambiguous gene descriptions), we used genome-wide BLAST searches with the respective predicted transcripts to search for other possible copies of the gene. We classified BLAST hits with >50% of the query and >70% identity as representing significant hits indicative of another copy of the gene. Genes with significant hits to the Z were classified as Z-W pairs, whereas those with no hits to the Z were classified as W unique, noting that some of the latter also showed other hits to the W and/or to some autosomes. Two of these were identified as members of a previously described zebra finch expansion of the PIM1L kinase gene (Kong et al., 2010), noting that they were previously unassigned to a chromosome as an assembled zebra finch W chromosome was then unavailable. Other cases could represent evidence of other gene duplications/expansions on the W and/or autosomes, but some could also represent repetitive elements and/or assembly artifacts. W unique genes were further assessed for evidence of expression in a range of zebra finch tissues based on publicly available transcriptome data mapped to W chromosome genes in the current zebra finch genome assembly and accessible through NCBI's RefSeq (Annotation release 106). We also assessed brain expression by *in situ* hybridization for two W genes with available ESTIMA clones (LOC116806961 and LOC116806962), noting that a possible sex difference for LOC116806962 may have been masked by nonspecific signal arising from shared domains with other PIM1L paralogs.

QUANTIFICATION AND STATISTICAL ANALYSIS

Differential gene expression—All code and custom functions used for RNA-seq analyses were written in R using RStudio and various Bioconductor packages (Friedrich, 2022). Briefly, STAR output tables were used to create a sample-by-gene count matrix. This count matrix was used as input to DESeq2 (v1.30G1) (Love et al., 2014), which performed filtering, normalization, and regularized log transformation. A sample PCA was generated based on variance transformed values. To determine significantly differentially expressed genes (DEGs), a negative binomial generalized linear model was fit to the data with sex and age as main factors with a sex + age interaction. Wald tests were performed on user-specified contrasts to determine: developmentally-regulated genes within each sex; sex-biased genes within each age; and genes significant for a sex + age interaction. To improve detection and diminish the multiple testing problem, independent filtering for each test was performed using the mean of normalized counts as a filter statistic. Genes with a Benjamini-Hochberg-based false discovery rate (FDR) < 0.01 were considered significant, and are referred to as DEGs. For visualization only, $\log_2$ fold change values were shrunk using the 'ashr' method (Stephens, 2017). Because none of the juveniles sang in the 20 min window between lights-on and sacrifice, we did not remove genes known to be singing-regulated (Dong et al., 2009; Mello and Clayton, 1994; Whitney et al., 2014) from our result sets.

Hierarchical clustering analysis—To identify groups of genes that showed similar differential expression profiles, we performed hierarchical clustering using the degPattern()

function from clusterProfiler (v3.18.1) (Yu et al., 2012). Only DEGs were considered and used as input for clustering analyses. From the regularized log transformed count matrix of relevant genes, the degPattern() function composes a distance matrix based on correlations between group means of gene expression, then constructs a hierarchy of clusterings based on that distance matrix.

Gene ontology (GO) analyses—To identify GO terms that were significantly enriched in our DEG sets, we used functions from clusterProfiler (v3.18.1) (Yu et al., 2012) to perform over-representation analysis (ORA) as well as gene set enrichment analysis (GSEA). Unlike ORA, GSEA does not require delineation of DEGs from non-differential genes. Instead, GSEA ranks the log-fold changes of all assessed genes to test for significantly coordinated shifts in gene pathways (Subramanian et al., 2005). Because these analytical tools are based on annotations that refer to human orthologs, zebra finch genes were mapped to their corresponding human orthologs based on HGNC symbol. For over-representation analyses, DEG sets were compared against a background of all assessed zebra finch genes with human orthologs in Ensembl (n = 11,541). Only enrichment terms with Benjamini-Hochberg adjusted p values < 0.05 and supported by at least 5 DEGs were considered. Excluded from this analysis were genes that could not be assigned to a human gene (n = 10,414), either due to differing gene symbols, or because there was no ortholog in the human genome. Thus, zebra finch-specific genes (e.g. as previously described in Wirthlin et al., 2014) are missing from these functional analyses.

Transcription factor binding site analysis—Genomic sequences and coordinates for all annotated zebra finch genes were obtained from NCBI (bTaeGut1_v1.p, Annotation Release 104) and sequences of interest (promoter regions defined as −1000 to +500 bp relative to the transcription start site) were then selected using custom Python code (Andrade and Velho, 2022b). To identify possible transcription factor binding sites (TFBS) in these sequences, we first identified 529 transcription factors (TFs) (Table S8) by searching gene descriptions for the phrase "transcription factor", as well as searching for genes annotated with GO:0003700 (DNA-binding transcription factor activity) among all DEGs and non DEGs identified in this study. We then retrieved all position weight matrices (PWMs) available in the JASPAR database (Portales-Casamar et al., 2010) for the TFs expressed in RA (339 out of 529), including 120 DEGs and 219 non-DEG TFs. To quantify the occurrence of potential TFBSs of both DEG and non-DEG TFs in DEG promoters, we used a scanning tool called FIMO (Find Individual Motif Occurrences; Grant et al., 2011), where genome subsequences and PWMs were integrated and transformed into a ranked list of motif occurrences. To evaluate the random effects of putative TFBS detection against a possible biological bias, we implemented a Monte Carlo analysis simulating samples with the same size as the DEG gene sets for each comparison, but with randomly selected genes from the entire set of assessed genes; a total of 20,000 simulations were run per each TF.

Supplementary Material

Refer to Web version on PubMed Central for supplementary material.

ACKNOWLEDGMENTS

REFERENCES

Adkins-Regan E, and Ascenzi M (1987). Social and sexual behaviour of male and female zebra finches treated with oestradiol during the nestling period. Anim. Behav. 35, 1100–1112. 10.1016/S0003-3472(87)80167-7.

Adkins-Regan E, Mansukhani V, Seiwert C, and Thompson R (1994). Sexual differentiation of brain and behavior in the zebra finch: critical periods for effects of early estrogen treatment. J. Neurobiol. 25, 865–877. 10.1002/neu.480250710. [PubMed: 8089662]

Adret P, and Margoliash D (2002). Metabolic and neural activity in the song system nucleus robustus archistriatalis: effect of age and gender. J. Comp. Neurol. 454, 409–423. 10.1002/cne.10459. [PubMed: 12455006]

Agate RJ, Grisham W, Wade J, Mann S, Wingfield J, Schanen C, Palotie A, and Arnold AP (2003). Neural, not gonadal, origin of brain sex differences in a gynandromorphic finch. Proc. Natl. Acad. Sci. USA 100, 4873–4878. 10.1073/pnas.0636925100. [PubMed: 12672961]

Akutagawa E, and Konishi M (1994). Two separate areas of the brain differentially guide the development of a song control nucleus in the zebra finch. Proc. Natl. Acad. Sci. USA 91, 12413–12417. 10.1073/pnas.91.26.12413. [PubMed: 7809051]

Akutagawa E, and Konishi M (1998). Transient expression and transport of brain-derived neurotrophic factor in the male zebra finch's song system during vocal development. Proc. Natl. Acad. Sci. USA 95, 11429–11434. 10.1073/pnas.95.19.11429. [PubMed: 9736753]

Andrade AL, and Velho TAF (2022a). VelhoLab/Monte-Carlo-Simulations- and-ZScore- Calculation: MonteCarlov1.0.0 (Zenodo). 10.5281/zenodo.6677897.

Andrade AL, and Velho TAF (2022b). VelhoLab/Query-NCBI-Promoter-Sequences-: PromoterSequenceRetrievalv1.0.0 (Zenodo). 10.5281/zenodo.6678104.

Andrews S (2010). FastQC: a quality control tool for high throughput sequence data. http://www.bioinformatics.babraham.ac.uk/projects/fastqc/.

Arnold AP (2009). The organizational–activational hypothesis as the foundation for a unified theory of sexual differentiation of all mammalian tissues. Horm. Behav. 55, 570–578. 10.1016/j.yhbeh.2009.03.011. [PubMed: 19446073]

Arnold AP, and Gorski RA (1984). Gonadal steroid induction of structural sex differences in the central nervous system. Annu. Rev. Neurosci. 7, 413–442. 10.1146/annurev.ne.07.030184.002213. [PubMed: 6370082]

Ball GF, Balthazart J, Fiasse V, and Absil P (1994). Effects of the aromatase inhibitor r76713 on sexual differentiation of brain and behavior in zebra finches. Behav. 131, 225–259.

Bloodgood BL, and Sabatini BL (2007). Nonlinear regulation of unitary synaptic signals by CaV(2.3) voltage-sensitive calcium channels located in dendritic spines. Neuron 53, 249–260. 10.1016/j.neuron.2006.12.017. [PubMed: 17224406]

Bolger AM, Lohse M, and Usadel B (2014). Trimmomatic: a flexible trimmer for Illumina sequence data. Bioinformatics 30, 2114–2120. 10.1093/bioinformatics/btu170. [PubMed: 24695404]

Bottjer SW, Miesner EA, and Arnold AP (1984). Forebrain lesions disrupt development but not maintenance of song in passerine birds. Science 224, 901–903. 10.1126/science.6719123. [PubMed: 6719123]

Bottjer SW, Glaessner SL, Arnold AP, and Arnold P (1985). Ontogeny of brain nuclei controlling song learning and behavior in zebra finches. J. Neurosci. 5, 1556–1562. [PubMed: 4009245]

Bottjer SW, Miesner EA, and Arnold AP (1986). Changes in neuronal number, density and size account for increases in volume of song-control nuclei during song development in zebra finches. Neurosci. Lett. 67, 263–268. 10.1016/0304-3940(86)90319-8. [PubMed: 3737014]

Brainard MS, and Doupe AJ (2002). What songbirds teach us about learning. Nature 417, 351–358. 10.1038/417351a. [PubMed: 12015616]

Braun K, Scheich H, Heizmann CW, and Hunziker W (1991). Parvalbumin and calbindin-D28K immunoreactivity as developmental markers of auditory and vocal motor nuclei of the zebra finch. Neuroscience 40, 853–869. 10.1016/0306-4522(91)90017-I. [PubMed: 2062443]

Burek MJ, Nordeen KW, and Nordeen EJ (1994). Ontogeny of sex differences among newly-generated neurons of the juvenile avian brain. Brain Res. Dev. Brain Res. 78, 57–64. 10.1016/0165-3806(94)90009-4. [PubMed: 8004774]

Carleton JB, Lovell PV, McHugh A, Marzulla T, Horback KL, and Mello CV (2014). An optimized protocol for high-throughput in situ hybridization of zebra finch brain. Cold Spring Harb. Protoc, 1249–1258. 10.1101/pdb.prot084582. [PubMed: 25342071]

Chen X, Agate RJ, Itoh Y, and Arnold AP (2005). Sexually dimorphic expression of trkB, a Z-linked gene, in early posthatch zebra finch brain. Proc. Natl. Acad. Sci. USA 102, 7730–7735. 10.1073/pnas.0408350102. [PubMed: 15894627]

Choe HN, Tewari J, Zhu KW, Davenport M, Matsunami H, and Jarvis ED (2021). Estrogen and sex-dependent loss of the vocal learning system in female zebra finches. Horm. Behav. 129, 104911. 10.1016/j.yhbeh.2020.104911. [PubMed: 33422557]

Clayton DF (1997). Role of gene regulation in song circuit development and song learning. J. Neurobiol. 33, 549–571. 10.1002/(SICI)1097-4695(19971105)33:5<549::AID-NEU5>3.0.CO;2-4. [PubMed: 9369459]

Clayton DF, George JM, Mello CV, and Siepka SM (2009). Conservation and expression of IQ-domain-containing calpacitin gene products (neuromodulin/GAP-43, neurogranin/RC3) in the adult and developing oscine song control system. Dev. Neurobiol. 69, 124–140. 10.1002/dneu.20686. [PubMed: 19023859]

Cooke B, Hegstrom CD, Villeneuve LS, and Breedlove SM (1998). Sexual differentiation of the vertebrate brain: principles and mechanisms. Front. Neuroendocrinol. 19, 323–362. 10.1006/frne.1998.0171. [PubMed: 9799588]

Curmi PA, Gavet O, Charbaut E, Ozon S, Lachkar-Colmerauer S, Manceau V, Siavoshian S, Maucuer A, and Sobel A (1999). Stathmin and its phosphoprotein family: general properties, biochemical and functional interaction with tubulin. Cell Struct. Funct. 24, 345–357. 10.1247/csf.24.345. [PubMed: 15216892]

DeWulf V, and Bottjer SW (2002). Age and sex differences in mitotic activity within the zebra finch telencephalon. J. Neurosci. 22, 4080–4094. 10.1523/JNEUROSCI.22-10-04080.2002. [PubMed: 12019327]

DeWulf V, and Bottjer SW (2005). Neurogenesis within the juvenile zebra finch telencephalic ventricular zone: a map of proliferative activity. J. Comp. Neurol. 481, 70–83. 10.1002/cne.20352. [PubMed: 15558733]

Dickson BJ (2002). Molecular mechanisms of axon guidance. Science 298, 1959–1964. 10.1126/science.1072165. [PubMed: 12471249]

Diddens J, Coussement L, Frankl-Vilches C, Majumdar G, Steyaert S, Ter Haar SM, Galle J, De Meester E, De Keulenaer S, Van Criekinge W, et al. (2021). DNA methylation regulates transcription factor-specific neurodevelopmental but not sexually dimorphic gene expression dynamics in zebra finch telencephalon. Front. Cell Dev. Biol. 9, 583555. 10.3389/fcell.2021.583555. [PubMed: 33816458]

Dittrich F, Feng Y, Metzdorf R, and Gahr M (1999). Estrogen-inducible, sex-specific expression of brain-derived neurotrophic factor mRNA in a forebrain song control nucleus of the juvenile zebra finch. Proc. Natl. Acad. Sci. USA 96, 8241–8246. 10.1073/pnas.96.14.8241. [PubMed: 10393979]

Dobin A, Davis CA, Schlesinger F, Drenkow J, Zaleski C, Jha S, Batut P, Chaisson M, and Gingeras TR (2013). STAR: ultrafast universal RNA-seq aligner. Bioinformatics 29, 15–21. 10.1093/bioinformatics/bts635. [PubMed: 23104886]

Dong S, Replogle KL, Hasadsri L, Imai BS, Yau PM, Rodriguez-Zas S, Southey BR, Sweedler JV, and Clayton DF (2009). Discrete molecular states in the brain accompany changing responses to a vocal signal. Proc. Natl. Acad. Sci. USA 106, 11364–11369. 10.1073/pnas.0812998106. [PubMed: 19541599]

Felbor U, Kessler B, Mothes W, Goebel HH, Ploegh HL, Bronson RT, and Olsen BR (2002). Neuronal loss and brain atrophy in mice lacking cathepsins B and L. Proc. Natl. Acad. Sci. USA 99, 7883–7888. 10.1073/pnas.112632299. [PubMed: 12048238]

Friedrich SR (2022). Samifriedrich/zebrafinchRA: v1.0.0 (v1.0.0) (Zenodo). 10.5281/zenodo.6639637.

Friedrich SR, Lovell PV, Kaser TM, and Mello CV (2019). Exploring the molecular basis of neuronal excitability in a vocal learner. BMC Genomics 20, 629. 10.1186/s12864-019-5871-2. [PubMed: 31375088]

Funkelstein L, Beinfeld M, Minokadeh A, Zadina J, and Hook V (2010). Unique biological function of cathepsin L in secretory vesicles for biosynthesis of neuropeptides. Neuropeptides 44, 457–466. 10.1016/j.npep.2010.08.003. [PubMed: 21047684]

Gahr M (1996). Developmental changes in the distribution of oestrogen receptor mRNA expressing cells in the forebrain of female, male and masculinized female zebra finches. Neuroreport 7, 2469–2473. [PubMed: 8981405]

George JM, Bell ZW, Condliffe D, Dohrer K, Abaurrea T, Spencer K, Leitão A, Gahr M, Hurd PJ, and Clayton DF (2019). Acute social isolation alters neurogenomic state in songbird forebrain. Proc. Natl. Acad. Sci. USA 117, 23311–23316. 10.1073/pnas.1820841116. [PubMed: 31332005]

González-Castillo C, Ortuño-Sahagún D, Guzmán-Brambila C, Pallàs M, and Rojas-Mayorquín AE (2015). Pleiotrophin as a central nervous system neuromodulator, evidences from the hippocampus. Front. Cell. Neurosci. 8, 443. 10.3389/fncel.2014.00443. [PubMed: 25620911]

Grant CE, Bailey TL, and Noble WS (2011). FIMO: scanning for occurrences of a given motif. Bioinformatics 27, 1017–1018. 10.1093/bioinformatics/btr064. [PubMed: 21330290]

Gunaratne PH, Lin Y-C, Benham AL, Drnevich J, Coarfa C, Tennakoon JB, Creighton CJ, Kim JH, Milosavljevic A, Watson M, et al. (2011). Song exposure regulates known and novel microRNAs in the zebra finch auditory forebrain. BMC Genomics 12, 277. 10.1186/1471-2164-12-277. [PubMed: 21627805]

Gurney ME (1981). Hormonal control of cell form and number in the zebra finch song system. J. Neurosci. 1, 658–673. 10.1523/JNEUROSCI.01-06-00658.1981. [PubMed: 7346574]

Gurney ME (1982). Behavioral correlates of sexual differentiation in the zebra finch song system. Brain Res. 231, 153–172. 10.1016/0006-8993(82)90015-4. [PubMed: 7055672]

Gurney ME, and Konishi M (1980). Hormone-induced sexual differentiation of brain and behavior in zebra finches. Science 208, 1380–1383. [PubMed: 17775725]

Hahnloser RHR, Kozhevnikov AA, and Fee MS (2002). An ultra-sparse code underlies the generation of neural sequences in a songbird. Nature 419, 65–70. 10.1038/nature00974. [PubMed: 12214232]

Herrmann K, and Arnold AP (1991). Lesions of HVC block the developmental masculinizing effects of estradiol in the female zebra finch song system. J. Neurobiol. 22, 29–39. 10.1002/neu.480220104. [PubMed: 2010748]

Hook V, Funkelstein L, Wegrzyn J, Bark S, Kindy M, and Hook G (2012). Cysteine cathepsins in the secretory vesicle produce active peptides: cathepsin L generates peptide neurotransmitters and cathepsin B produces beta-amyloid of Alzheimer's disease. Biochim. Biophys. Acta 1824, 89–104. 10.1016/j.bbapap.2011.08.015. [PubMed: 21925292]

Itoh Y, Melamed E, Yang X, Kampf K, Wang S, Yehya N, Van Nas A, Replogle K, Band MR, Clayton DF, et al. (2007). Dosage compensation is less effective in birds than in mammals. J. Biol. 6, 2. 10.1186/jbiol53. [PubMed: 17352797]

Itoh Y, Replogle K, Kim Y-H, Wade J, Clayton DF, and Arnold AP (2010). Sex bias and dosage compensation in the zebra finch versus chicken genomes: general and specialized patterns among birds. Genome Res. 20, 512–518. 10.1101/gr.102343.109. [PubMed: 20357053]

Jacobs EC, Arnold AP, and Campagnoni AT (1999). Developmental regulation of the distribution of aromatase- and estrogen-receptor- mRNA-expressing cells in the zebra finch brain. Dev. Neurosci. 21, 453–472. 10.1159/000017413. [PubMed: 10640864]

Janik VM, and Knörnschild M (2021). Vocal production learning in mammals revisited. Philos. Trans. R. Soc. Lond. B Biol. Sci. 376, 20200244. 10.1098/rstb.2020.0244. [PubMed: 34482736]

Jarvis ED (2019). Evolution of vocal learning and spoken language. Science 366, 50–54. 10.1126/science.aax0287. [PubMed: 31604300]

Johnson F, and Bottjer SW (1994). Afferent influences on cell death and birth during development of a cortical nucleus necessary for learned vocal behavior in zebra finches. Development 120, 13–24. [PubMed: 21375056]

Johnson F, Hohmann SE, DiStefano PS, and Bottjer SW (1997). Neurotrophins suppress apoptosis induced by deafferentation of an avian motor-cortical region. J. Neurosci. 17, 2101–2111. 10.1523/JNEUROSCI.17-06-02101.1997. [PubMed: 9045737]

Kim Y-H, Perlman WR, and Arnold AP (2004). Expression of androgen receptor mRNA in zebra finch song system: developmental regulation by estrogen. J. Comp. Neurol. 469, 535–547. 10.1002/cne.11033. [PubMed: 14755534]

Kimpo RR, and Doupe AJ (1997). FOS is induced by singing in distinct neuronal populations in a motor network. Neuron 18, 315–325. 10.1016/s0896-6273(00)80271-8. [PubMed: 9052801]

Kirn JR, and DeVoogd TJ (1989). Genesis and death of vocal control neurons during sexual differentiation in the zebra finch. J. Neurosci. 9, 3176–3187. [PubMed: 2795159]

Ko M-C, Frankl-Vilches C, Bakker A, and Gahr M (2021). The gene expression profile of the song control nucleus HVC shows sex specificity, hormone responsiveness, and species specificity among songbirds. Front. Neurosci. 15, 680530. 10.3389/fnins.2021.680530. [PubMed: 34135731]

Kong L, Lovell PV, Heger A, Mello CV, and Ponting CP (2010). Accelerated evolution of PAK3- and PIM1-like kinase gene families in the zebra finch, Taeniopygia guttata. Mol. Biol. Evol. 27, 1923–1934. 10.1093/molbev/msq080. [PubMed: 20237222]

Konishi M, and Akutagawa E (1985). Neuronal growth, atrophy and death in a sexually dimorphic song nucleus in the zebra finch brain. Nature 315, 145–147. 10.1038/315145a0. [PubMed: 3990816]

Konishi M, and Akutagawa E (1987). Hormonal control of cell death in a sexually dimorphic song nucleus in the zebra finch. In Novartis Foundation Symposia, Bock G and O'Connor M, eds. (John Wiley & Sons, Ltd.), pp. 173–185.

Leonardo A, and Fee MS (2005). Ensemble coding of vocal control in birdsong. J. Neurosci. 25, 652–661. 10.1523/JNEUROSCI.3036-04.2005. [PubMed: 15659602]

Lin Y-C, Balakrishnan CN, and Clayton DF (2014). Functional genomic analysis and neuroanatomical localization of miR-2954, a song-responsive sex-linked microRNA in the zebra finch. Front. Neurosci. 8, 409. 10.3389/fnins.2014.00409. [PubMed: 25565940]

Love MI, Huber W, and Anders S (2014). Moderated estimation of fold change and dispersion for RNA-seq data with DESeq2. Genome Biol. 15, 550. 10.1186/s13059-014-0550-8. [PubMed: 25516281]

Lovell PV, Wirthlin M, Kaser T, Buckner AA, Carleton JB, Snider BR, McHugh AK, Tolpygo A, Mitra PP, and Mello CV (2020). ZEBrA: zebra finch Expression Brain Atlas—a resource for comparative molecular neuroanatomy and brain evolution studies. J. Comp. Neurol. 528, 2099–2131. 10.1002/cne.24879. [PubMed: 32037563]

Mccarthy M, De Vries G, and Forger N (2017). Sexual differentiation of the brain: a fresh look at mode, mechanisms, and meaning. In Hormones, Brain and Behavior, PFaff DW and Joëls M, eds. (Academic Press), pp. 3–32.

McCarthy MM, Pickett LA, VanRyzin JW, and Kight KE (2015). Surprising origins of sex differences in the brain. Horm. Behav. 76, 3–10. 10.1016/j.yhbeh.2015.04.013. [PubMed: 25917865]

Mello CV, and Clayton DF (1994). Song-induced ZENK gene expression in auditory pathways of songbird brain and its relation to the song control system. J. Neurosci. 14, 6652–6666. 10.1523/JNEUROSCI.14-11-06652.1994. [PubMed: 7965067]

Mello CV, Vicario DS, and Clayton DF (1992). Song presentation induces gene expression in the songbird forebrain. Proc. Natl. Acad. Sci. USA 89, 6818–6822. 10.1073/pnas.89.15.6818. [PubMed: 1495970]

Merten MD, and Stocker-Buschina S (1995). Fadrozole induces delayed effects on neurons in the zebra finch song system. Brain Res. 671, 317–320. 10.1016/0006-8993(94)01370-W. [PubMed: 7743222]

Mooney R, and Rao M (1994). Waiting periods versus early innervation: the development of axonal connections in the zebra finch song system. J. Neurosci. 14, 6532–6543. [PubMed: 7965057]

Morgan CP, and Bale TL (2012). Sex differences in microRNA regulation of gene expression: no smoke, just miRs. Biol. Sex Differ. 3, 22. 10.1186/2042-6410-3-22. [PubMed: 23009289]

Mori C, and Wada K (2015). Audition-independent vocal crystallization associated with intrinsic developmental gene expression dynamics. J. Neurosci. 35, 878–889. 10.1523/JNEUROSCI.1804-14.2015. [PubMed: 25609608]

Nevue AA, Lovell PV, Wirthlin M, and Mello CV (2020). Molecular specializations of deep cortical layer analogs in songbirds. Sci. Rep. 10, 18767. 10.1038/s41598-020-75773-4. [PubMed: 33127988]

Nixdorf-Bergweiler BE (1996). Divergent and parallel development in volume sizes of telencephalic song nuclei in male and female zebra finches. J. Comp. Neurol. 375, 445–456. 10.1002/(SICI)1096-9861(19961118)375:3<445::AID-CNE7>3.0.CO;2-2. [PubMed: 8915841]

Nordeen EJ, and Nordeen KW (1988a). Sex and regional differences in the incorporation of neurons born during song learning in zebra finches. J. Neurosci. 8, 2869–2874. 10.1523/JNEUROSCI.08-08-02869.1988. [PubMed: 3411358]

Nordeen EJ, and Nordeen KW (1996). Sex difference among nonneuronal cells precedes sexually dimorphic neuron growth and survival in an avian song control nucleus. J. Neurobiol. 30, 531–542. 10.1002/(SICI)1097-4695(199608)30:4<531::AID-NEU8>3.0.CO;2-4. [PubMed: 8844516]

Nordeen KW, and Nordeen EJ (1988b). Projection neurons within a vocal motor pathway are born during song learning in zebra finches. Nature 334, 149–151. 10.1038/334149a0. [PubMed: 3386754]

Nordeen EJ, Grace A, Burek MJ, and Nordeen KW (1992). Sex-dependent loss of projection neurons involved in avian song learning. J. Neurobiol. 23, 671–679. 10.1002/neu.480230606. [PubMed: 1279116]

Nordeen EJ, Voelkel L, and Nordeen KW (1998). Fibroblast growth factor-2 stimulates cell proliferation and decreases sexually dimorphic cell death in an avian song control nucleus. J. Neurobiol. 37, 573–581. 10.1002/(SICI)1097-4695(199812)37:4<573::AID-NEU6>3.0.CO;2-6. [PubMed: 9858259]

Nottebohm F, Stokes TM, and Leonard CM (1976). Central control of song in the canary, Serinus canarius. J. Comp. Neurol. 165, 457–486. 10.1002/cne.901650405. [PubMed: 1262540]

Nottebohm F, Kelley DB, and Paton JA (1982). Connections of vocal control nuclei in the canary telencephalon. J. Comp. Neurol. 207, 344–357. 10.1002/cne.902070406. [PubMed: 7119147]

Ohkawa N, Fujitani K, Tokunaga E, Furuya S, and Inokuchi K (2007). The microtubule destabilizer stathmin mediates the development of dendritic arbors in neuronal cells. J. Cell Sci. 120, 1447–1456. 10.1242/jcs.001461. [PubMed: 17389683]

Ölveczky BP, Otchy TM, Goldberg JH, Aronov D, and Fee MS (2011). Changes in the neural control of a complex motor sequence during learning. J. Neurophysiol. 106, 386–397. 10.1152/jn.00018.2011. [PubMed: 21543758]

Paradis E, Julien P, and Ven Murthy MR (2004). Requirement for enzymatically active lipoprotein lipase in neuronal differentiation: a site-directed mutagenesis study. Brain Res. Dev. Brain Res. 149, 29–37. 10.1016/j.devbrainres.2003.12.003. [PubMed: 15013626]

Pohl-Apel G, and Sossinka R (1984). Hormonal determination of song capacity in females of the zebra finch: critical phase of treatment. Z. Tierpsychol. 64, 330–336. 10.1111/j.1439-0310.1984.tb00367.x.

Portales-Casamar E, Thongjuea S, Kwon AT, Arenillas D, Zhao X, Valen E, Yusuf D, Lenhard B, Wasserman WW, and Sandelin A (2010). JASPAR 2010: the greatly expanded open-access database of transcription factor binding profiles. Nucleic Acids Res. 38, D105–D110. 10.1093/nar/gkp950. [PubMed: 19906716]

Radhakrishnan B, and Alwin Prem Anand A (2016). Role of miRNA-9 in brain development. J. Exp. Neurosci. 10, 101–120. 10.4137/JEN.S32843. [PubMed: 27721656]

Replogle K, Arnold AP, Ball GF, Band M, Bensch S, Brenowitz EA, Dong S, Drnevich J, Ferris M, George JM, et al. (2008). The Songbird Neurogenomics (SoNG) Initiative: community-based tools and strategies for study of brain gene function and evolution. BMC Genomics 9, 131. 10.1186/1471-2164-9-131. [PubMed: 18366674]

Ruminot I, Schmälzle J, Leyton B, Barros LF, and Deitmer JW (2019). Tight coupling of astrocyte energy metabolism to synaptic activity revealed by genetically encoded FRET nanosensors in hippocampal tissue. J. Cereb. Blood Flow Metab. 39, 513–523. 10.1177/0271678X17737012. [PubMed: 29083247]

Scharff C, and Nottebohm F (1991). A comparative study of the behavioral deficits following lesions of various parts of the zebra finch song system: implications for vocal learning. J. Neurosci. 11, 2896–2913. [PubMed: 1880555]

Shaughnessy DW, Hyson RL, Bertram R, Wu W, and Johnson F (2019). Female zebra finches do not sing yet share neural pathways necessary for singing in males. J. Comp. Neurol. 527, 843–855. 10.1002/cne.24569. [PubMed: 30370534]

Shi Z, Zhang Z, Schaffer L, Huang Z, Fu L, Head S, Gaasterland T, Wang X, and Li X (2021). Dynamic transcriptome landscape in the song nucleus HVC between juvenile and adult zebra finches. Adv. Genet. 2, e10035. 10.1002/ggn2.10035.

Simpson HB, and Vicario DS (1991a). Early estrogen treatment alone causes female zebra finches to produce learned, male-like vocalizations. J. Neurobiol. 22, 755–776. 10.1002/neu.480220710. [PubMed: 1765782]

Simpson HB, and Vicario DS (1991b). Early estrogen treatment of female zebra finches masculinizes the brain pathway for learned vocalizations. J. Neurobiol. 22, 777–793. 10.1002/neu.480220711. [PubMed: 1765783]

Soderstrom K, Qin W, and Leggett MH (2007). A minimally invasive procedure for sexing young zebra finches. J. Neurosci. Methods 164, 116–119. 10.1016/j.jneumeth.2007.04.007. [PubMed: 17532050]

Sohrabji F, Nordeen EJ, and Nordeen KW (1990). Selective impairment of song learning following lesions of a forebrain nucleus in the juvenile zebra finch. Behav. Neural. Biol. 53, 51–63. 10.1016/0163-1047(90)90797-a. [PubMed: 2302141]

Song H, and Poo M (2001). The cell biology of neuronal navigation. Nat. Cell Biol. 3, E81–E88. 10.1038/35060164. [PubMed: 11231595]

Stahl S, Reinders Y, Asan E, Mothes W, Conzelmann E, Sickmann A, and Felbor U (2007). Proteomic analysis of cathepsin B and L-deficient mouse brain lysosomes. Biochim. Biophys. Acta 1774, 1237–1246. 10.1016/j.bbapap.2007.07.004. [PubMed: 17765022]

Stephens M (2017). False discovery rates: a new deal. Biostatistics 18, 275–294. 10.1093/biostatistics/kxw041. [PubMed: 27756721]

Subramanian A, Tamayo P, Mootha VK, Mukherjee S, Ebert BL, Gillette MA, Paulovich A, Pomeroy SL, Golub TR, Lander ES, and Mesirov JP (2005). Gene set enrichment analysis: a knowledge-based approach for interpreting genome-wide expression profiles. Proc. Natl. Acad. Sci. USA 102, 15545–15550. 10.1073/pnas.0506580102. [PubMed: 16199517]

Tang YP, and Wade J (2011). Developmental changes in the sexually dimorphic expression of secretory carrier membrane protein 1 and its co-localisation with androgen receptor protein in the zebra finch song system. J. Neuroendocrinol. 23, 584–590. 10.1111/j.1365-2826.2011.02146.x. [PubMed: 21518034]

Tang YP, and Wade J (2016). Sex and age differences in brain-derived neurotrophic factor and vimentin in the zebra finch song system: relationships to newly generated cells. J. Comp. Neurol. 524, 1081–1096. 10.1002/cne.23893. [PubMed: 26355496]

Tang C, Wang M, Wang P, Wang L, Wu Q, and Guo W (2019). Neural stem cells behave as a functional niche for the maturation of newborn neurons through the secretion of PTN. Neuron 101, 32–44.e6. 10.1016/j.neuron.2018.10.051. [PubMed: 30497772]

Tohda C, and Tohda M (2017). Extracellular cathepsin L stimulates axonal growth in neurons. BMC Res. Notes 10, 613. 10.1186/s13104-017-2940-y. [PubMed: 29169406]

Tomaszycki ML, Peabody C, Replogle K, Clayton DF, Tempelman RJ, and Wade J (2009). Sexual differentiation of the zebra finch song system: potential roles for sex chromosome genes. BMC Neurosci. 10, 24. 10.1186/1471-2202-10-24. [PubMed: 19309515]

Velho TAF, Lovell P, and Mello CV (2007). Enriched expression and developmental regulation of the middle-weight neurofilament (NF-m) gene in song control nuclei of the zebra finch. J. Comp. Neurol. 500, 477–497. 10.1002/cne.21180. [PubMed: 17120287]

Vicario DS (1991). Organization of the zebra finch song control system: functional organization of outputs from nucleus robustus archistriatalis. J. Comp. Neurol. 309, 486–494. 10.1002/cne.903090405. [PubMed: 1655832]

Vidak E, Javoršek U, Vizovišek M, and Turk B (2019). Cysteine cathepsins and their extracellular roles: shaping the microenvironment. Cells 8, 264. 10.3390/cells8030264.

de Vries GJ (2004). Minireview: sex differences in adult and developing brains: compensation, compensation, compensation. Endocrinology 145, 1063–1068. 10.1210/en.2003-1504. [PubMed: 14670982]

Wada K, Howard JT, McConnell P, Whitney O, Lints T, Rivas MV, Horita H, Patterson MA, White SA, Scharff C, et al. (2006). A molecular neuroethological approach for identifying and characterizing a cascade of behaviorally regulated genes. Proc. Natl. Acad. Sci. USA 103, 15212–15217. 10.1073/pnas.0607098103. [PubMed: 17018643]

Wade J, and Arnold AP (2004). Sexual differentiation of the zebra finch song system. Ann. N. Y. Acad. Sci. 1016, 540–559. 10.1196/annals.1298.015. [PubMed: 15313794]

Wade J, Swender DA, and McElhinny TL (1999). Sexual differentiation of the zebra finch song system parallels genetic, not gonadal, sex. Horm. Behav. 36, 141–152. 10.1006/hbeh.1999.1537. [PubMed: 10506538]

Wade J, Tang YP, Peabody C, and Tempelman RJ (2005). Enhanced gene expression in the forebrain of hatchling and juvenile male zebra finches. J. Neurobiol. 64, 224–238. 10.1002/neu.20141. [PubMed: 15849735]

Wang J, Sakaguchi H, and Sokabe M (1999). Sex differences in the vocal motor pathway of the zebra finch revealed by real-time optical imaging technique. Neuroreport 10, 2487–2491. [PubMed: 10574357]

Wang K, Kelley MH, Wu WW, Adelman JP, and Maylie J (2015a). Apamin boosting of synaptic potentials in CaV2.3 R-type Ca2+ channel null mice. PLoS One 10, e0139332. 10.1371/journal.pone.0139332. [PubMed: 26418566]

Wang R, Chen C-C, Hara E, Rivas MV, Roulhac PL, Howard JT, Chakraborty M, Audet J-N, and Jarvis ED (2015b). Convergent differential regulation of SLIT-ROBO axon guidance genes in the brains of vocal learners. J. Comp. Neurol. 523, 892–906. 10.1002/cne.23719. [PubMed: 25424606]

Watabe-Uchida M, John KA, Janas JA, Newey SE, and Van Aelst L (2006). The Rac activator DOCK7 regulates neuronal polarity through local phosphorylation of stathmin/Op18. Neuron 51, 727–739. 10.1016/j.neuron.2006.07.020. [PubMed: 16982419]

Whitney O, Pfenning AR, Howard JT, Blatti CA, Liu F, Ward JM, Wang R, Audet J-N, Kellis M, Mukherjee S, et al. (2014). Core and region-enriched networks of behaviorally regulated genes and the singing genome. Science 346, 1256780. 10.1126/science.1256780. [PubMed: 25504732]

Wild JM, Williams MN, and Suthers RA (2001). Parvalbumin-positive projection neurons characterise the vocal premotor pathway in male, but not female, zebra finches. Brain Res. 917, 235–252. [PubMed: 11640910]

Wirthlin M, Lovell PV, Jarvis ED, and Mello CV (2014). Comparative genomics reveals molecular features unique to the songbird lineage. BMC Genomics 15, 1082. 10.1186/1471-2164-15-1082. [PubMed: 25494627]

Yu AC, and Margoliash D (1996). Temporal hierarchical control of singing in birds. Science 273, 1871–1875. 10.1126/science.273.5283.1871. [PubMed: 8791594]

Yu G, Wang L-G, Han Y, and He Q-Y (2012). clusterProfiler: an R package for comparing biological themes among gene clusters. OMICS 16, 284–287. 10.1089/omi.2011.0118. [PubMed: 22455463]

Zann R (1996). The Zebra Finch: A Synthesis of Field and Laboratory Studies (Oxford University Press).

Zemel BM, Nevue AA, Dagostin A, Lovell PV, Mello CV, and von Gersdorff H (2021). Resurgent Na+ currents promote ultrafast spiking in projection neurons that drive fine motor control. Nat. Commun. 12, 6762. 10.1038/s41467-021-26521-3. [PubMed: 34799550]

Highlights

- Transcriptomic divergence in the RA mirrors the extent of the RA's sexual dimorphism

- RA transcriptome dynamics follow distinctly sex-specific developmental trajectories

- Early dominance of Z-linked sex differences switches later to autosomal differences

- Transcription factor analyses point to pro-apoptotic regulatory networks in females
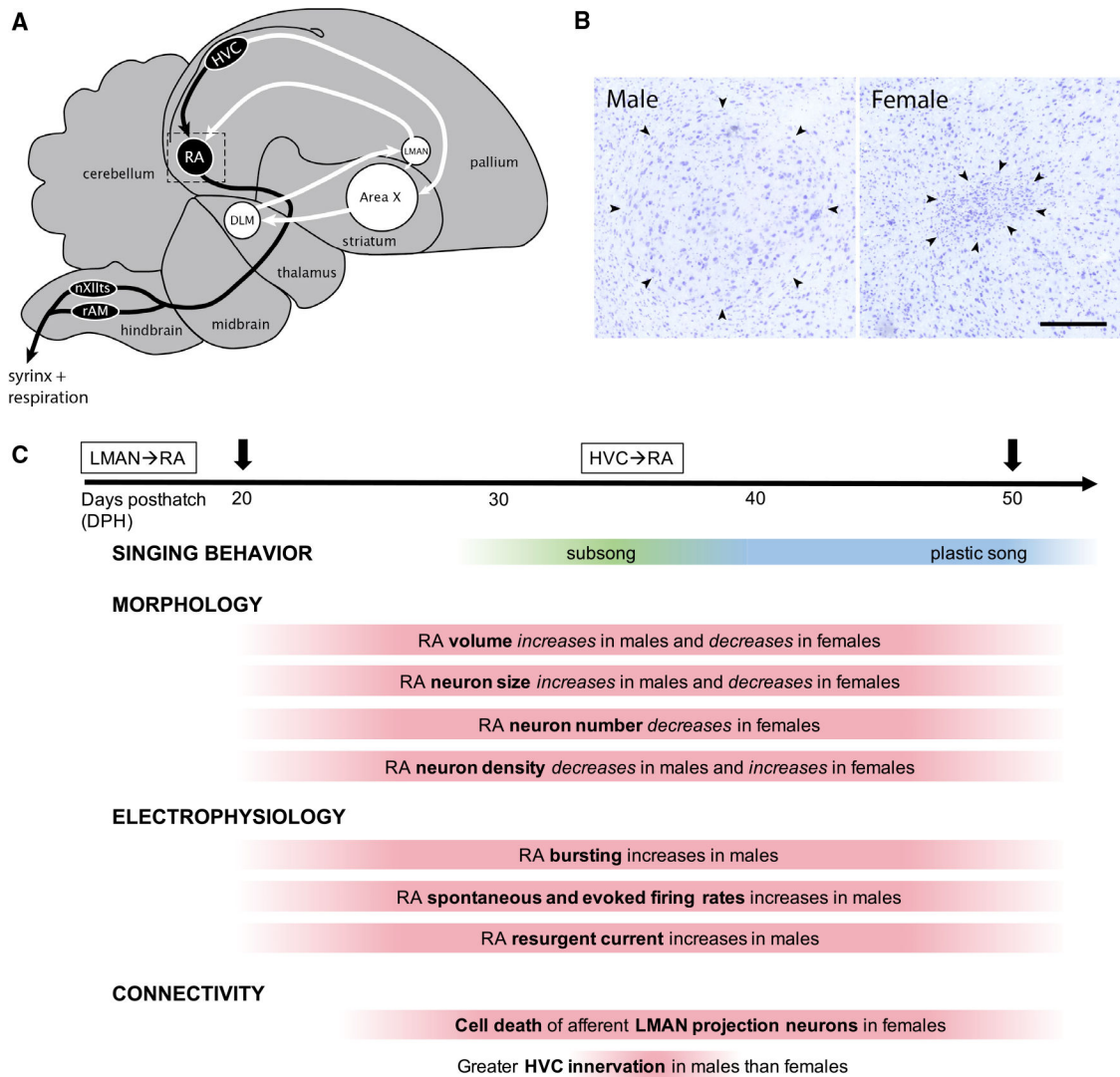
Figure 1. Sexually dimorphic development of the song nucleus RA

(A) A simplified schematic of the song nuclei and their connections, shown from a parasagittal view. Note that not all connections are shown. Black fills indicate the direct motor pathway (DMP) and white fills indicate the anterior forebrain pathway (AFP). Black dashed box indicates area shown in (B) and in the *in situ* hybridization images shown in Figures 3D and 4B. Abbreviations: HVC, proper name; LMAN, lateral magnocellular nucleus of the anterior nidopallium; RA, robust nucleus of the arcopallium; Area X, proper name; DLM, dorsal lateral nucleus of the medial thalamus; nXIIts, motor nucleus of the tracheosyringeal part of the XIIth cranial nerve; rAM, nucleus retroambigualis medialis.

(B) Nissl stains of parasagittal 10 μm brain sections from adult zebra finches showing RA (indicated by arrowheads) and surrounding arcopallium. Scale bar, 250 μm.

(C) Developmental timeline of sex differences in the RA. Text boxes (top) denote approximate timing of afferent innervation from the RA's main afferents LMAN and HVC. Arrows denote ages used to generate RNA-seq data for this study; for the corresponding Nissl images, see Figure S1. Information summarized from Adret and Margoliash (2002),

Bottjer et al. (1985, 1986), Burek et al. (1994), Kirn and DeVoogd (1989), Konishi and Akutagawa (1985, 1987), Mooney and Rao (1994), Nixdorf-Bergweiler (1996), Nordeen and Nordeen (1988a, 1988b), Nordeen et al. (1992), Ölveczky et al. (2011), Zemel et al. (2021).
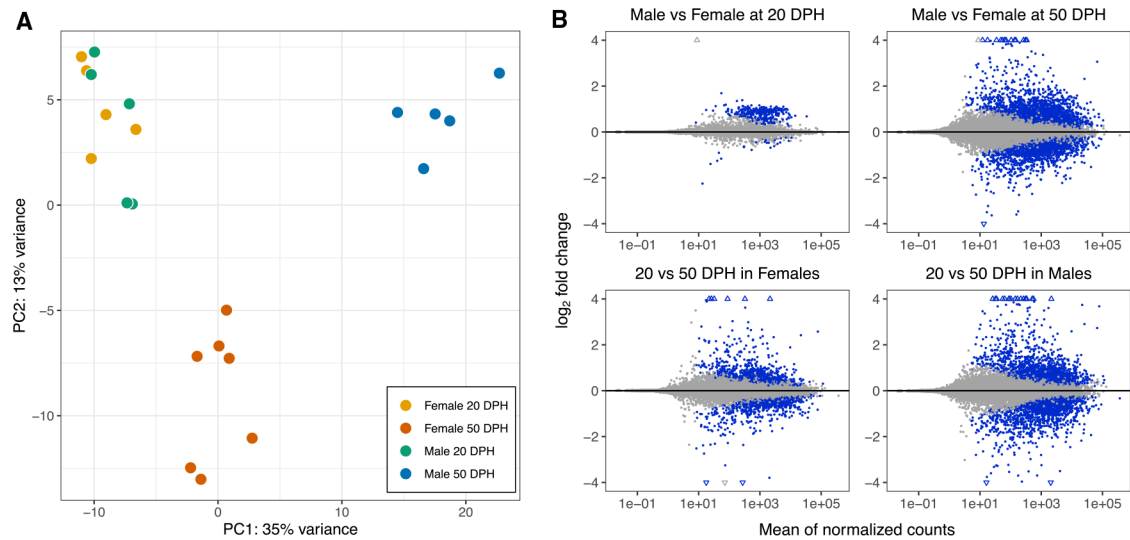
Figure 2. Sex-specific developmental changes in RA transcriptome

(A) PCA plot of all RNA-seq samples. The 500 most variant genes were used to calculate principal components (PCs), and the first two PCs are plotted. Sample group is indicated by color. The 20 DPH male (green) and female (yellow) samples cluster together, while the 50 DPH samples cluster by sex (female, orange; male, blue). For a PCA plot of all RNA-seq samples based on all assessed genes (n = 21,955), see Figure S2.

(B) MA plots of DEGs for sex and age contrasts. Positive $\log_2$ fold-change values indicate higher expression in males for sex contrasts (top) and higher expression at 50 DPH in age contrasts (bottom). Negative values indicate higher expression in females (top) and at 20 DPH (bottom). Blue and gray points represent differential and nondifferential genes, respectively. Triangles represent genes with $\log_2$ fold changes >|4|. Log$_2$ fold-change values were shrunk for visualization using the "ashr" method (Stephens, 2017). The differential expression statistics for all genes examined is presented in Table S1. For an examination of DEGs in male development that are known RA markers published in the Zebra Finch Expression Brain Atlas, ZEBrA (Lovell et al., 2020), see Table S2.
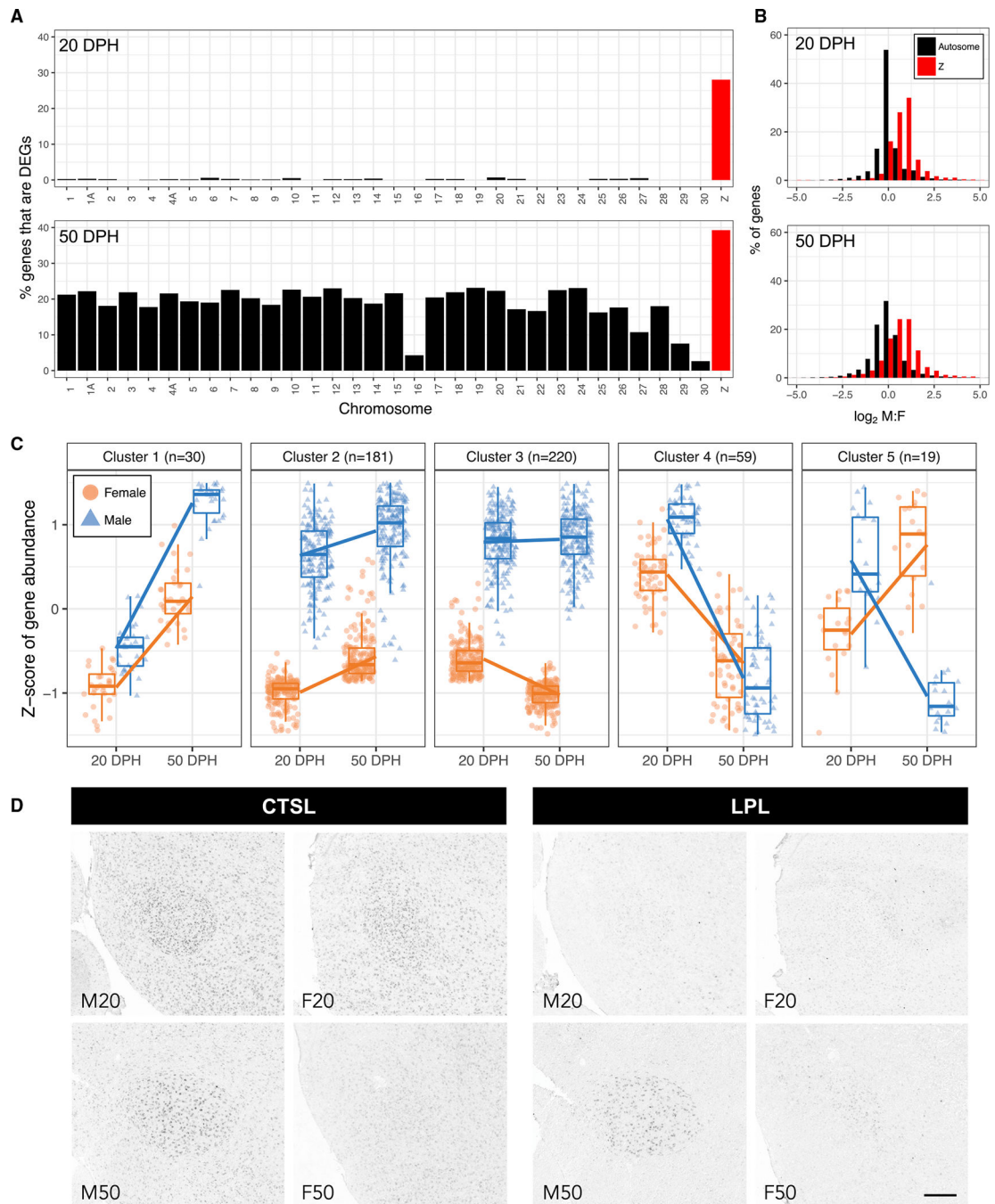
Figure 3. Sex and age differences in RA expression of autosomal and Z-linked genes

(A) Sex-biased genes by chromosome at 20 and 50 DPH. Number of DEGs per chromosome was normalized to the total number of genes on each chromosome to account for differences in chromosome length and gene density.

(B) Histograms of sex-biased expression ($\log_2$ M:F) for all genes on autosomes (black) and the Z chromosome (red) at 20 and 50 DPH.

(C) Expression pattern clustering for all Z-chromosome DEGs. Points denote values for individual genes and are left-right jittered to prevent overplotting; box plots denote group

median values (thick horizontal lines), 25th to 75th percentiles (box bounds), and most extreme values up to 1.5 times the interquartile range (vertical whiskers); diagonal lines connect mean group values across age in each sex. Number of genes per cluster is displayed above each plot.

(D) Expression of sex-differential chromosome Z genes in the developing RA. Shown are *in situ* hybridization photomicrographs of parasagittal sections at the core of the RA. Scale bar, 250 μm. The ESTIMA clones used for riboprobes were CTSL (cathepsin L), DV957210, and LPL (lipoprotein lipase), CK313328. For curation of W-chromosome genes, see Table S3; for evidence of brain expression of a W-chromosome gene, see Figure S3A; for LPL expression in the adult male RA, see Figure S3B.
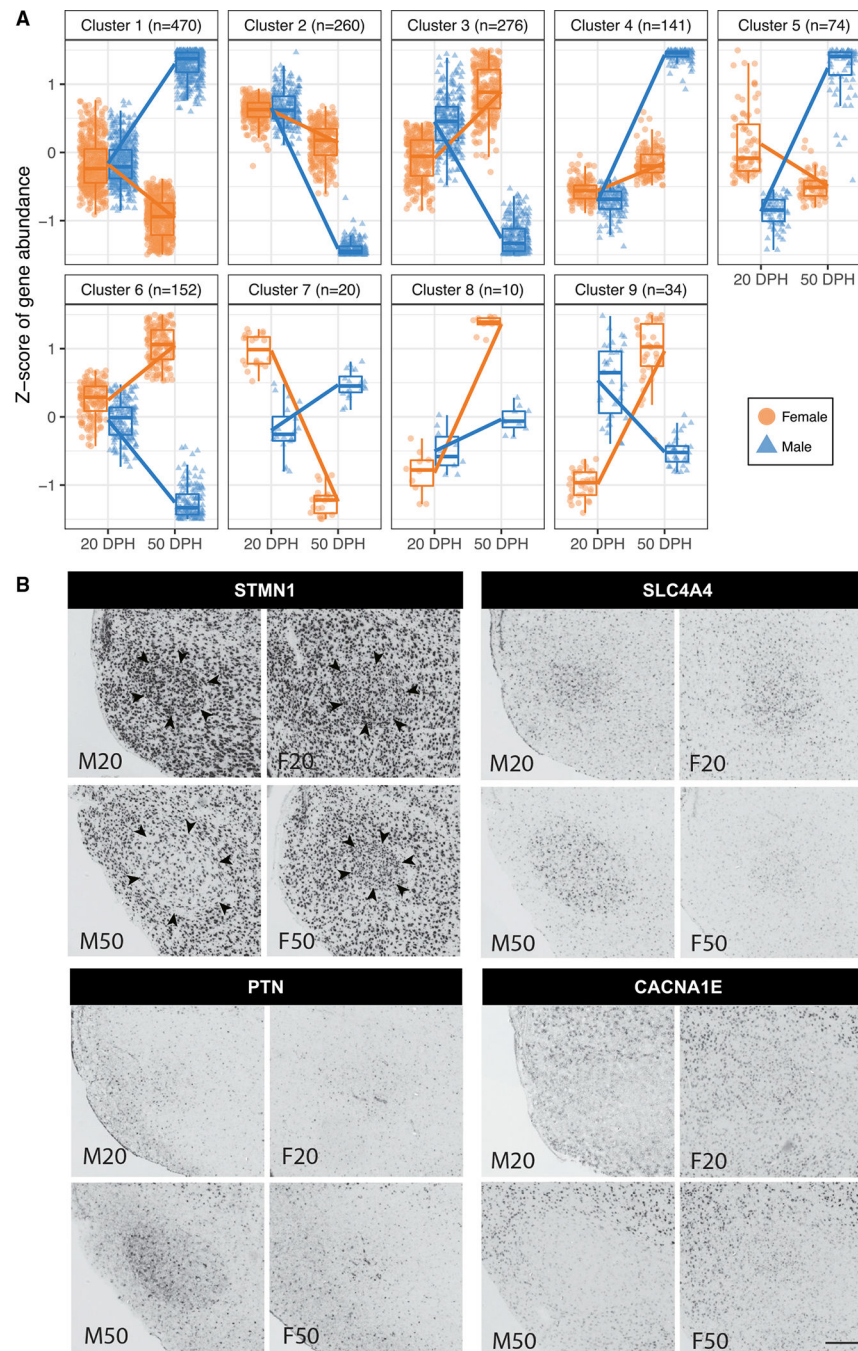
Figure 4. Sex and age differences in RA expression of DEGs that show an interaction between sex and age

(A) Expression pattern clustering for DEGs that were significant for an interaction between sex and age. Plot explanation is as in Figure 3C. Number of genes in each cluster is displayed above each plot.

(B) Expression of genes significant for an interaction between sex and age in the developing RA. Shown are *in situ* hybridization photomicrographs of parasagittal sections at the core of RA. Scale bar, 250 μm. The ESTIMA clones used for riboprobes were STMN1 (stathmin 1), CK311233; SLC4A4 (solute carrier family 4 member 4), CK305917; PTN (pleiotrophin),

CK314329; and CACNA1E (calcium voltage-gated channel subunit α1 E), FE728835. For overrepresentation analysis (ORA) of GO terms for sex + age interaction DEG clusters, see Table S7.

Author Manuscript

Author Manuscript
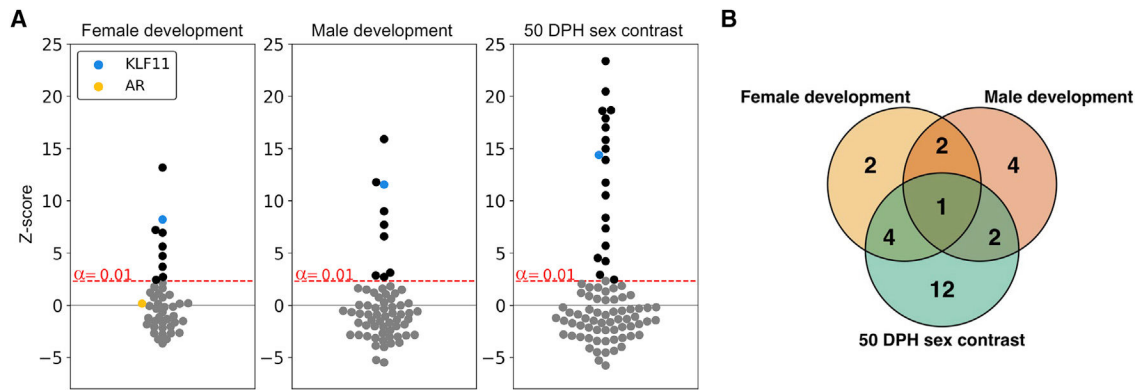
Author Manuscript

Author Manuscript

Figure 5. Transcription factor binding site analysis of DEG transcription factors

(A) Transcription factor binding site (TFBS) enrichments in female development (left), male development (middle), and 50 DPH sex contrast (right) DEG sets. DEG transcription factors with significantly enriched binding sites are shown in black, except for KLF11 (blue); DEG transcription factors with no significant enrichment of binding sites are shown in gray, except for androgen receptor (AR; orange). Red dashed line denotes statistical signficance boundary.

(B) Venn diagram depicts overlaps in DEG transcription factors with enriched TFBSs from all contrasts in (A). Only one DEG transcription factor (KLF11) shows TFBS enrichment in all DEG contrast sets. For other overlapping sets, see Table S9. For further details on the KLF11 TFBS, see Figures S4A and S4B. For TFBS analysis of non-DEG transcription factors, see Figure S4C. For the full list of identified DEG TFs, see Table S8 ("transcription factors" tab). For evidence of female-specific developmental increase in expression of AR, see Figure S5.

Table 1.

Summary of GO enrichments for female RA development

Cell movement	
GO:0051271	negative regulation of cellular component movement
GO:0030336	negative regulation of cell migration
Regulation of membrane potential	
GO:1903817	negative regulation of voltage-gated potassium channel activity
GO:1902260	negative regulation of delayed rectifier potassium channel activity
Cell differentiation	
GO:0010001	glial cell differentiation
GO:0048709	oligodendrocyte differentiation
GO:0045666	positive regulation of neuron differentiation
GO:0045165	cell fate commitment
Cell polarity	
GO:0032878	regulation of establishment or maintenance of cell polarity
GO:2000114	regulation of establishment of cell polarity
GO:0007163	establishment or maintenance of cell polarity
GO:0045197	establishment or maintenance of epithelial cell apical/basal polarity
Transcriptional regulation	
GO:0001217	DNA-binding transcription repressor activity
GO:0035195	gene silencing by miRNA
GO:0150100	RNA binding involved in posttranscriptional gene silencing
GO:0001216	DNA-binding transcription activator activity
Hormone signaling	
GO:0048545	response to steroid hormone
GO:0009755	hormone-mediated signaling pathway

Immune signaling

GO:0001817	regulation of cytokine production
GO:0001816	cytokine production
GO:0002449	lymphocyte-mediated immunity
GO:0002706	regulation of lymphocyte-mediated immunity

See Tables S4, S5, and S6 for detailed results.

Table 2.

Summary of GO enrichments for male RA development

Cell movement	
GO:0042330	taxis

Regulation of membrane potential	
GO:0042391	regulation of membrane potential
GO:0034765	regulation of ion transmembrane transport
GO:0005244	voltage-gated ion channel activity
GO:0046873	metal ion transmembrane transporter activity
GO:0017080	sodium channel regulator activity

Axon and projection development	
GO:0061564	axon development
GO:0014003	oligodendrocyte development
GO:0031346	positive regulation of cell projection organization
GO:0032291	axon ensheathment in central nervous system
GO:0043217	myelin maintenance
GO:1990138	neuron projection extension

Synapse assembly, organization, and activity	
GO:0050808	synapse organization
GO:0051963	regulation of synapse assembly
GO:0050803	regulation of synapse structure or activity
GO:0099560	synaptic membrane adhesion
GO:0099177	regulation of *trans*-synaptic signaling
GO:0051937	catecholamine transport
GO:0099601	regulation of neurotransmitter receptor activity
GO:1900449	regulation of glutamate receptor signaling pathway
GO:0099003	vesicle-mediated transport in synapse
GO:0099645	neurotransmitter receptor localization to postsynaptic specialization membrane

Cell growth and morphogenesis

GO:0022604	regulation of cell morphogenesis
GO:0060560	developmental growth involved in morphogenesis
GO:0061387	regulation of extent of cell growth
GO:0048588	developmental cell growth

Cell energetics and metabolism

GO:0006734	NADH metabolic process
GO:0009150	purine ribonucleotide metabolic process
GO:0006091	generation of precursor metabolites and energy
GO:0006090	pyruvate metabolic process
GO:0046034	ATP metabolic process
GO:0061718	glucose catabolic process to pyruvate
GO:0019693	ribose phosphate metabolic process
GO:0044282	small-molecule catabolic process
GO:0010563	negative regulation of phosphorus metabolic process
GO:0016052	carbohydrate catabolic process

See Tables S4, S5, and S6 for detailed results.

KEY RESOURCES TABLE

REAGENT or RESOURCE	SOURCE	IDENTIFIER
Antibodies		
Anti-Digoxigenin-AP, Fab fragments	Roche	Cat#11093274910; RRID:AB_514497
Chemicals, peptides, and recombinant proteins		
RNase Away	Thermo Scientific	Cat#7000TS1
Chelex 100 Chelating Resin, 200–400 mesh	Bio-Rad Laboratories	Cat#1421253
Platinum Taq DNA Polymerase	Invitrogen	Cat#10966018
2-mercaptoethanol	Sigma-Aldrich	Cat#M3148
DIG RNA Labeling Mix	Roche	Cat#11277073910
Triethanolamine	Fisher	Cat#T350
Formamide	Fisher	Cat#F84
BCIP/NBT	Perkin-Elmer	Cat#NEL937
Acetic Anhydride	Sigma	Cat#A6404
Triton X-100	Sigma	Cat#T8787
BSSHII	NEB	Cat#R0199S
T3 RNA Polymerase	Promega	Cat#P208C
Critical commercial assays		
RNeasy Micro Kit	Qiagen	Cat#74004
RNA 6000 Pico Kit	Agilent	Cat#5067–1513
SmartSeq v4 PLUS kit	Takara Bio USA	Cat#R400752
PEN membrane glass slides	Leica	Cat#11505158
RLT buffer	Qiagen	Cat#79216
QIAquick PCR Purification Kit	Qiagen	Cat#28104
QIAprep Spin Miniprep Kit	Qiagen	Cat#27104
Deposited data		
bTaeGut1_v1.p *Taeniopygia guttata* assembly	NCBI	GCF_003957565.1

REAGENT or RESOURCE	SOURCE	IDENTIFIER
Taeniopygia guttata Annotation Release 104	NCBI	https://www.ncbi.nlm.nih.gov/genome/annotation_euk/Taeniopygia_guttata/104/
Human reference genome NCBI build 38, GRCh38	Genome Reference Consortium	http://www.ncbi.nlm.nih.gov/projects/genome/assembly/grc/human/
Emergence of sex-specific transcriptomes in a sexually-dimorphic brain nucleus	Gene Expression Omnibus (GEO)	GSE191296
Experimental models: Organisms/strains		
Zebra finch (*Taeniopygia guttata castanotis*)	Mello lab (OHSU) and Magnolia Bird Farm (Riverside, CA)	N/A
Oligonucleotides		
W-Forward: GGGTTTTGACTGACTAACTGATT	Soderstrom et al., (2007)	N/A
W-Reverse: GTTCAAAGCTACATGAATAAACA	Soderstrom et al., (2007)	N/A
Z-Forward: GTGTAGTCCGCTGCTTTTGG	Soderstrom et al., (2007)	N/A
Z-Reverse: GTTCGTGGTCTTCCACGTTT	Soderstrom et al., (2007)	N/A
Recombinant DNA		
ESTIMA collection of zebra finch brain cDNA clones used for riboprobe synthesis for *in situ* hybridizations	NCBI and Replogle et al. (2008)	N/A
Software and algorithms		
trimmomatic (v0.36)	Bolger et al. (2014)	http://www.usadellab.org/cms/?page=trimmomatic
FastQC (v0.11.9)	Andrews (2010)	https://www.bioinformatics.babraham.ac.uk/projects/fastqc/
Splice-aware STAR (v2.6.1)	Dobin et al. (2013)	https://github.com/alexdobin/STAR
R code and custom functions used for RNA-seq analyses	This paper	https://doi.org/10.5281/zenodo.6639637
DESeq2 (v1.30.1)	Love et al. (2014)	https://bioconductor.org/packages/release/bioc/html/DESeq2.html
ashr	Stephens (2017)	https://github.com/stephens999/ashr
clusterProfiler (v3.18.1)	Yu et al. (2012)	https://bioconductor.org/packages/release/bioc/html/clusterProfiler.html
FIMO (Find Individual Motif Occurrences)	Grant et al., (2011).	https://meme-suite.org/meme/doc/fimo.html
Code used for TF matrices analysis and Monte Carlo simulation	This paper	https://doi.org/10.5281/zenodo.6677897
Code used for promoter sequence retrieval	This paper	https://doi.org/10.5281/zenodo.6678104